C

U. S. ARMY

TRANSPORTATION RESEARCH COMMAND
FORT EUSTIS, VIRGINIA

PRELIMINARY FLIGHT TEST DATA

XH-51A RIGID ROTOR HIGH SPEED FLIGHT PROGRAM

INTERIM REPORT NO. 9

DECEMBER 1964

CLEARINGHOUSE FOR FEDERAL SCIENTIFIC AND TECHNICAL INFORMATION, CFSTI
INPUT SECTION 410.11

LIMITATIONS IN REPRODUCTION QUALITY OF TECHNICAL ABSTRACT BULLETIN DOCUMENTS, DEFENSE DOCUMENTATION CENTER (DDC)

AD621893

☐ 1. AVAILABLE ONLY FOR REFERENCE USE AT DDC FIELD SERVICES. COPY IS NOT AVAILABLE FOR PUBLIC SALE.

☒ 2. AVAILABLE COPY WILL NOT PERMIT FULLY LEGIBLE REPRODUCTION. REPRODUCTION WILL BE MADE IF REQUESTED BY USERS OF DDC.

☒ A. COPY IS AVAILABLE FOR PUBLIC SALE.

☐ B. COPY IS NOT AVAILABLE FOR PUBLIC SALE.

☐ 3. LIMITED NUMBER OF COPIES CONTAINING COLOR OTHER THAN BLACK AND WHITE ARE AVAILABLE UNTIL STOCK IS EXHAUSTED. REPRODUCTIONS WILL BE MADE IN BLACK AND WHITE ONLY.

TSL-121-2/65

DATE PROCESSED: 10/18/65

PROCESSOR: ASutton

SUMMARY

This report summarizes the flight test results of the Phase IV, XH-51A compound helicopter testing. For this program, an XH-51A helicopter was modified to incorporate a wing and a J-60 auxiliary jet engine. The purpose of this phase was to obtain flight test data on performance, stability, maneuverability, critical stresses and vibration at speeds up to an objective of 200 knots. The data included in this report presents the results in these areas at speeds up to a level flight true airspeed of 210 knots.

The completion of this phase represents the end of the flight testing required by the original contract. Preparation of a final report is in progress.

Results and Discussion

Performance

Level flight performance of the compound helicopter in terms of shaft horsepower required is shown on Figure 1. This data has been corrected to sea level standard day and shows performance as a pure helicopter, with the J-60 engine at idle and in full compound flight. Figure 2 shows the jet thrust required for the same flight condition. Figure 3 shows the tail rotor power required. Equivalent total propulsive power requirement can be seen by summing the curves shown in Figures 1, 2, and 3. Figure 4 shows the variation of rotor lift which was measured during the performance testing. Note that at the high speeds the rotor was very nearly unloaded.

Flying Qualities

Cyclic control stick positions in trimmed level flight are shown on Figure 5. During the course of the program, the incidence of the control gyro arms was reduced from 30 degrees to 5 degrees to reduce structural loads in the gyro drive system. This resulted in a change in the aerodynamic forces which produce a gyro processing moment and an apparent shift in the static stick-fixed longitudinal stability. Actual longitudinal stability, evidenced by the pitching moment of the wing-body against the rotor system was not altered by the gyro arm incidence change.

As forward flight speed was increased, measurement of the one per rev. flapwise bending in the main rotor, resolved to show the pitching and rolling components, indicated increasingly negative longitudinal stability. To restore positive longitudinal stability, the size of the horizontal tailplane was increased. Figures 6 and 7 show the effect of the change in area of the horizontal tailplane on the pitching component of the main rotor one per revolution flapwise bending.

Tail rotor pedal position is shown in figure 8 and indicates that ample directional control margins existed at high speed.

Maneuvering stability was comfortably positive throughout the test program. This is shown on Figure 9.

Structures:

Structural measurements including loads in the main rotor hub and blades, control gyro arms, main rotor pitch link, tail rotor, horizontal stabilizer, wing bending, and main rotor lift were obtained. A review of the loads measured indicates that the major structural item most likely to govern the fatigue life of the vehicle is the main rotor hub at station 7.0. Hub flapwise and chordwise bending moments were measured at hub station 6. These station 6 bending moments can be converted to stress at station 7 by the following factors.

Station 6 flapwise bending moment, inch pounds X 1.42 = station 7 stress, psi

Station 6 chordwise bending moment, inch pounds X 0.152 = station 7 stress, psi

Assuming a stress concentration factor of 3, the hub at station 7 has an estimated endurance limit cyclic stress of 26,000 psi.

The compound helicopter was initially flown without the auxiliary J-60 jet engine operating. These tests were conducted from hover to a forward speed of 96 knots CAS. The structural loads with the J-60 off are shown in Figures 10 and 11. The structural loads on these plots are essentially the same as the conventional XH-51A helicopter loads extrapolated to the weight and C.G. of the compound helicopter.

The next series of tests were conducted with the J-60 at idle (approximately 200 pounds of thrust). The structural loads with the J-60 at idle are shown in Figures 10 and 12. These plots show that the main rotor hub loads decrease with the added thrust from the J-60 at idle. With increased J-60 thrust for level flight, tests were conducted to determine the optimum collective blade angle setting for the higher speeds. The structural loads are plotted versus collective blade angle for the various speeds and collective blade settings up to 158 knots CAS, Figures 13, 14, and 15. From these tests, the optimum collective blade angle setting from a blade loads standpoint was determined to be approximately 4.5 degrees. The main rotor hub loads for this collective blade angle setting are also plotted versus calibrated airspeed on Figure 10.

With the large horizontal stabilizer at zero degree incidence, tests were conducted at 120 knots and 140 knots with variations in collective to determine the effect of collective blade angle setting. The data from these tests are plotted in Figures 16, 17, and 18. Extrapolation of these data to the higher speed conditions indicated that a collective setting around 3.8 degrees would be a satisfactory compromise angle for proceeding to high speeds with a constant collective blade angle.

The speed was built up to 201.5 knots CAS in approximately 10 knot increments with the collective blade angle held at approximately 3.8 degrees. The data from these tests are plotted versus airspeed in Figures 19 through 23.

The main rotor blade flapwise cyclic bending at station 6 shown in Figure 19 increased almost linearly with speed to a maximum value of 15,300 inch pounds at 201.5 knots. As can be seen in Figure 23, the majority of this moment was caused by the one per revolution pitch and roll components of the blade bending.

The cyclic flapwise bending at station 6 of 15,300 inch pounds converts to a cyclic stress of 21,700 psi at station 7. The cyclic chordwise moment at station 6 of 18,200 inch pounds converts to a stress of 2,800 psi at station 7. The sum of the two results in a maximum possible cyclic stress of 24,500 psi as compated to an estimated endurance limit of 26,000 psi.

Main rotor pitch link axial loads are shown in Figure 21. The maximum cyclic loads are only 137 pounds as compared to an estimated endurance limit of 1,400 pounds. Note that there has been no tendency for the loads to increase rapidly with speed increase. The blade feathering and torsion loads have increased only very gradually with increase in airspeed.

Gyro arm flap and chord bending loads also are shown in Figure 21. At speeds above 170 knots, the gyro arm incidence angle setting was reduced from 30 degrees to 5 degrees. This had negligible effect on the cyclic chordwise loads, but did reduce the cyclic flapwise loads. The incidence angle was changed to reduce the steady torsion load on the gyro drive shaft. The cyclic loads measured are well below the estimated endurance limit of the gyro arm.

Measurements of tail rotor flapwise bending at station 19.5 were obtained at speeds above 170 knots. These are shown in Figure 22. Analysis of data obtained during previous tests with the three-blade main rotor had shown that station 19.5 was the most critical bending station on the tail rotor. The cyclic loads fall somewhat below what might be expected by extrapolating the measurements as a regular helicopter; however, they are approaching the estimated endurance limit of 790 inch pounds. Linear extrapolation of the data indicates that the endurance limit would be reached at a speed somewhere between 230 and 240 knots CAS.

Measured horizontal stabilizer bending loads are shown in Figure 20. There is a difference between the average load L and R indicating an apparent swirl in the air flow in that area. The static loads are well under the limit static strength. The cyclic loads obtained are reasonably high and the frequency of motion is at tail rotor rotational frequency. The symmetrical first bending mode of the stabilizer, as determined by ground shake tests, is 30.5 cps. The tail rotor rotatational frequency is 35 cps and apparently the two frequencies are close enough together to provide a reasonable amount of excitation to the stabilizer. To help alleviate this, cable guy wires were strung from the stabilizer tips to the fuselage top and bottom at the stabilizer. These helped keep the oscillatory amplitude from building up too rapidly. The estimated endurance

limit for the stabilizer is 3,200 inch pounds. This was exceeded by 22 per cent for a few minutes of flight time in the runs at speeds above 180 knots.

Autorotation Entries

Structural loads during the transition from powered flight to autorotation and during the autorotation are usually less than experienced in powered level flight and therefore are not shown.

Maneuvering Conditions

The load factors obtained at various airspeeds with the J-60 jet engine off are shown in Figure 24. The maximum speed obtained with jet off was 134 knots CAS and the maximum load factor was 1.51 g's with the minimum load factor of 0.4 g's. With the jet engine operating, the speed-load factor values obtained are plotted in Figure 25. The maximum load factor obtained was 1.8 g's and the minimum 0.64 g's. All load factors are corrected to a weight of 4,300 pounds.

Main rotor flapwise and chordwise bending moments at station 6 and flapwise bending moment at station 157 are plotted versus load factor in Figures 26, 27, and 28. With the jet engine on and the collective blade angle lowered, the flapwise average bending moments at station 6 are more negative due to the reduced rotor lift. The cyclic loads scatter considerably and do not appear to have any significant trend with either load factor or rotor lift. With reduced rotor lift, the chordwise loads, both average and cyclic, are reduced considerably at all load factors. At station 157, the flapwise cyclic bending loads appear to be somewhat smaller with a reduced collective blade angle (jet engine on), whereas the average loads appear to be relatively unaffected by the collective blade angle.

The flapwise and chordwise cyclic loads are the maximum loads that occurred during the maneuver and do not necessarily occur at the time of the maximum load factor.

Vibration

Cabin vibration levels are shown on Figure 10 for the pure helicopter mode and Figure 11 with the J-60 at idle. Due to the high gross weight and the power levels required, these vibration levels are excessive.

In compound flight, the vibration levels are greatly reduced and are shown on Figure 29 for frequencies of 4 per revolution and higher.

DATA INDEX
PHASE IV

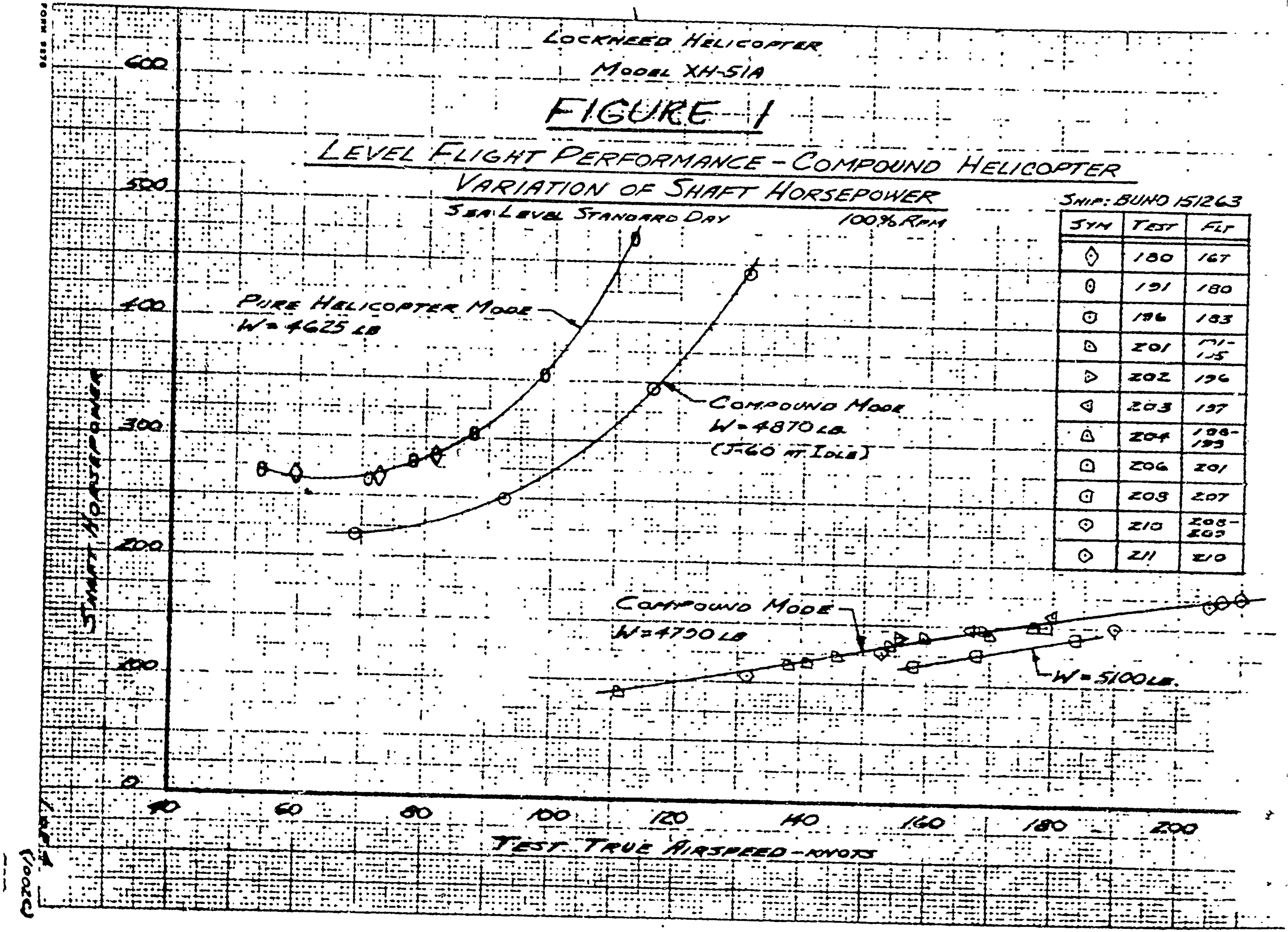

LOCKHEED HELICOPTER
MODEL XH-51A
FIGURE 1
LEVEL FLIGHT PERFORMANCE - COMPOUND HELICOPTER
VARIATION OF SHAFT HORSEPOWER
SEA LEVEL STANDARD DAY
100% RPM
SHIP: BUNO 151263
SYM TEST FLT
180 167
191 180
196 183
201 171-175
202 196
203 197
204 198-199
206 201
208 207
210 208-209
211 210
PURE HELICOPTER MODE
W = 4625 LB
COMPOUND MODE
W = 4870 LB
(J-60 AT IDLE)
COMPOUND MODE
W = 4790 LB
W = 5100 LB.
SHAFT HORSEPOWER
0
100
200
300
400
500
600
40
60
80
100
120
140
160
180
200
TEST TRUE AIRSPEED - KNOTS

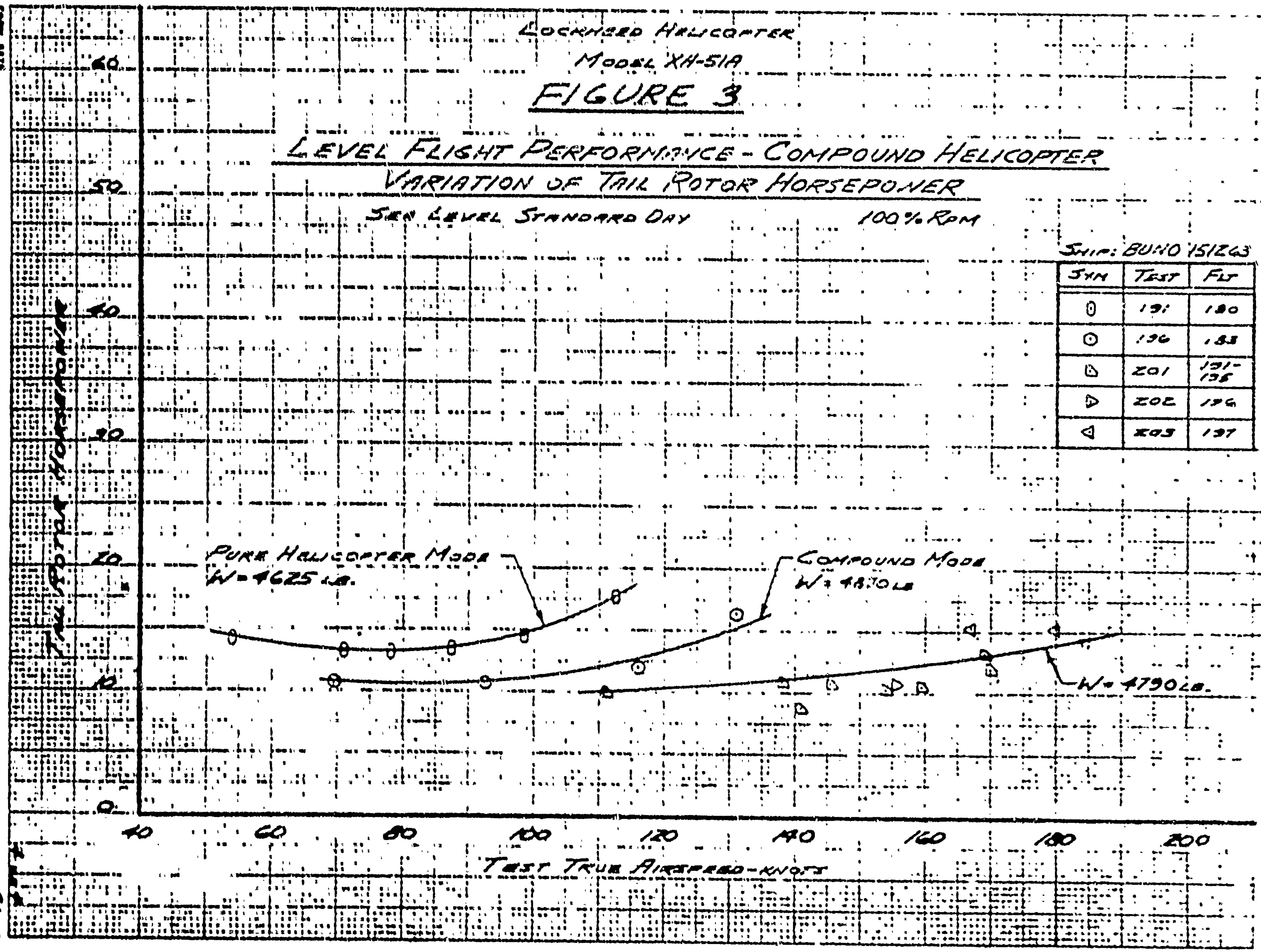
LOCKHEED HELICOPTER
MODEL XH-51A
FIGURE 3
LEVEL FLIGHT PERFORMANCE - COMPOUND HELICOPTER
VARIATION OF TAIL ROTOR HORSEPOWER
SEA LEVEL STANDARD DAY
100% RPM
SHIP: BUNO 151263
SYM | TEST | FLT
191 | 180
196 | 183
201 | 131-135
202 | 136
203 | 137
PURE HELICOPTER MODE
W=4625 LB.
COMPOUND MODE
W=4870 LB
W=4790 LB.
TAIL ROTOR HORSEPOWER
0
10
20
30
40
50
60
40
60
80
100
120
140
160
180
200
TEST TRUE AIRSPEED-KNOTS

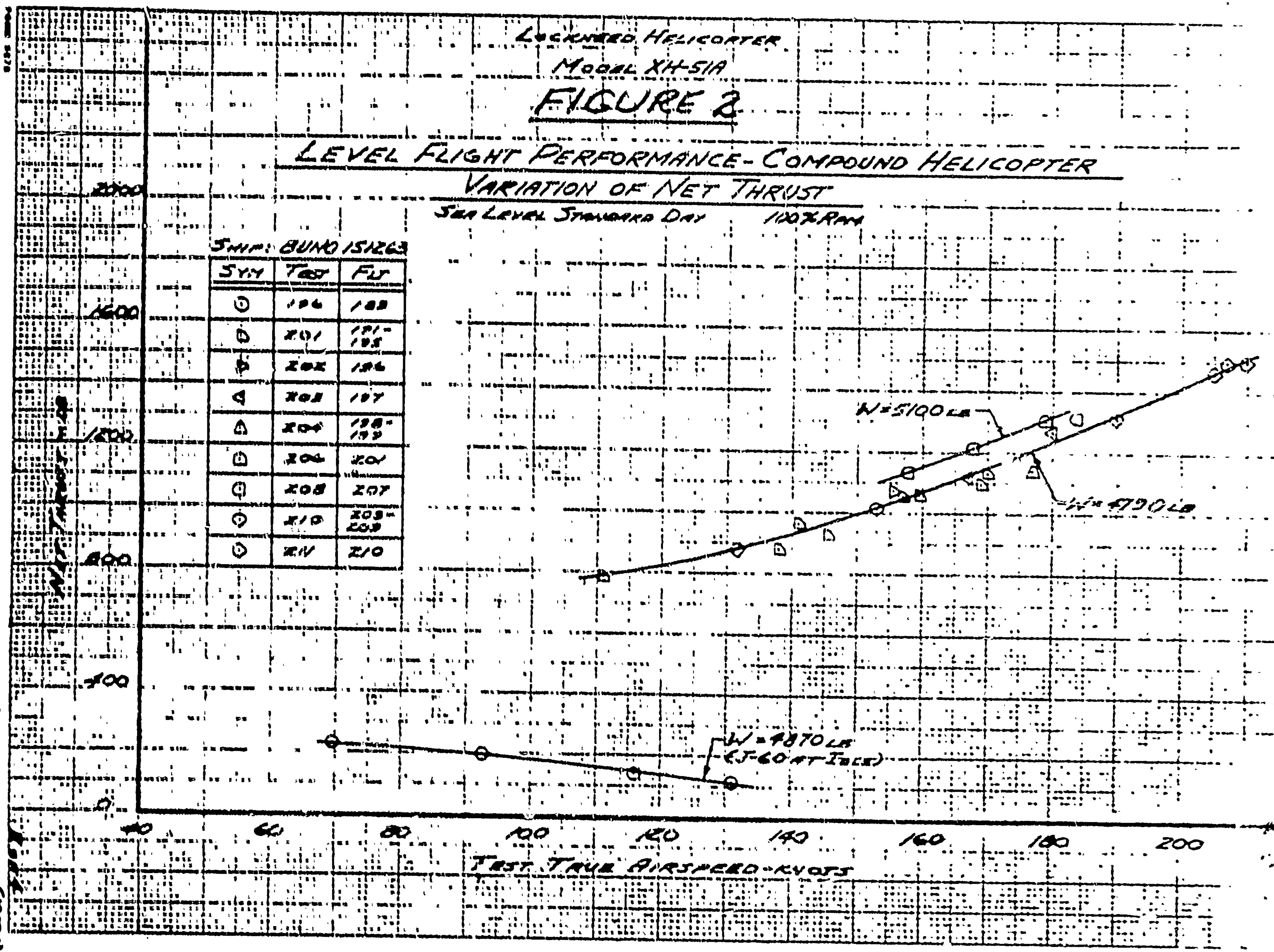

LOCKHEED HELICOPTER
MODEL XH-51A
FIGURE 2
LEVEL FLIGHT PERFORMANCE - COMPOUND HELICOPTER
VARIATION OF NET THRUST
SEA LEVEL STANDARD DAY
100% RPM
SHIP: BUNO 151263
SYM TEST FLT
196 188
201 191-195
202 196
203 197
204 198-199
206 201
208 207
210 203-209
214 210
W=5100 LB
W=4790 LB
W=4870 LB
(J-60 AT IDLE)
NET THRUST - LB
0
400
800
1200
1600
2000
40
60
80
100
120
140
160
180
200
TEST TRUE AIRSPEED - KNOTS

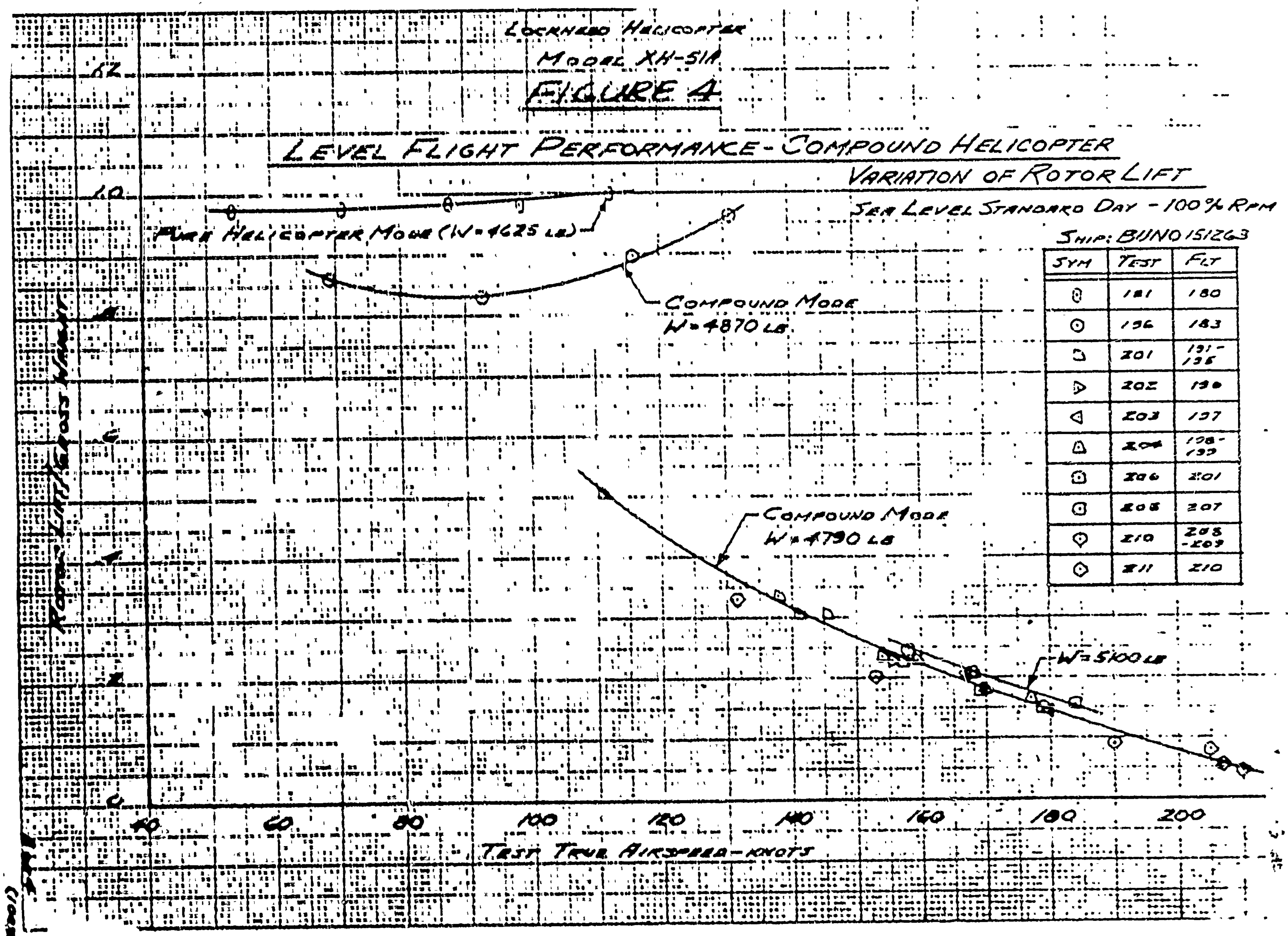
Lockheed Helicopter
Model XH-51A
FIGURE 4
Level Flight Performance - Compound Helicopter
Variation of Rotor Lift
Sea Level Standard Day - 100% RPM
Ship: BUNO 151263
Pure Helicopter Mode (W=4625 LB)
Compound Mode W=4870 LB
Compound Mode W=4790 LB
W=5100 LB
Rotor Lift/Gross Weight
Test True Airspeed - Knots
SYM TEST FLT
181 180
156 183
201 191-195
202 196
203 197
204 198-199
206 201
205 207
210 208-209
211 210

LOCKHEED HELICOPTER
MODEL XH-51A
SHIP - BUNO 151263

CYCLIC CONTROL POSITIONS IN LEVEL FLIGHT

COMPOUND HELICOPTER

FIGURE 5

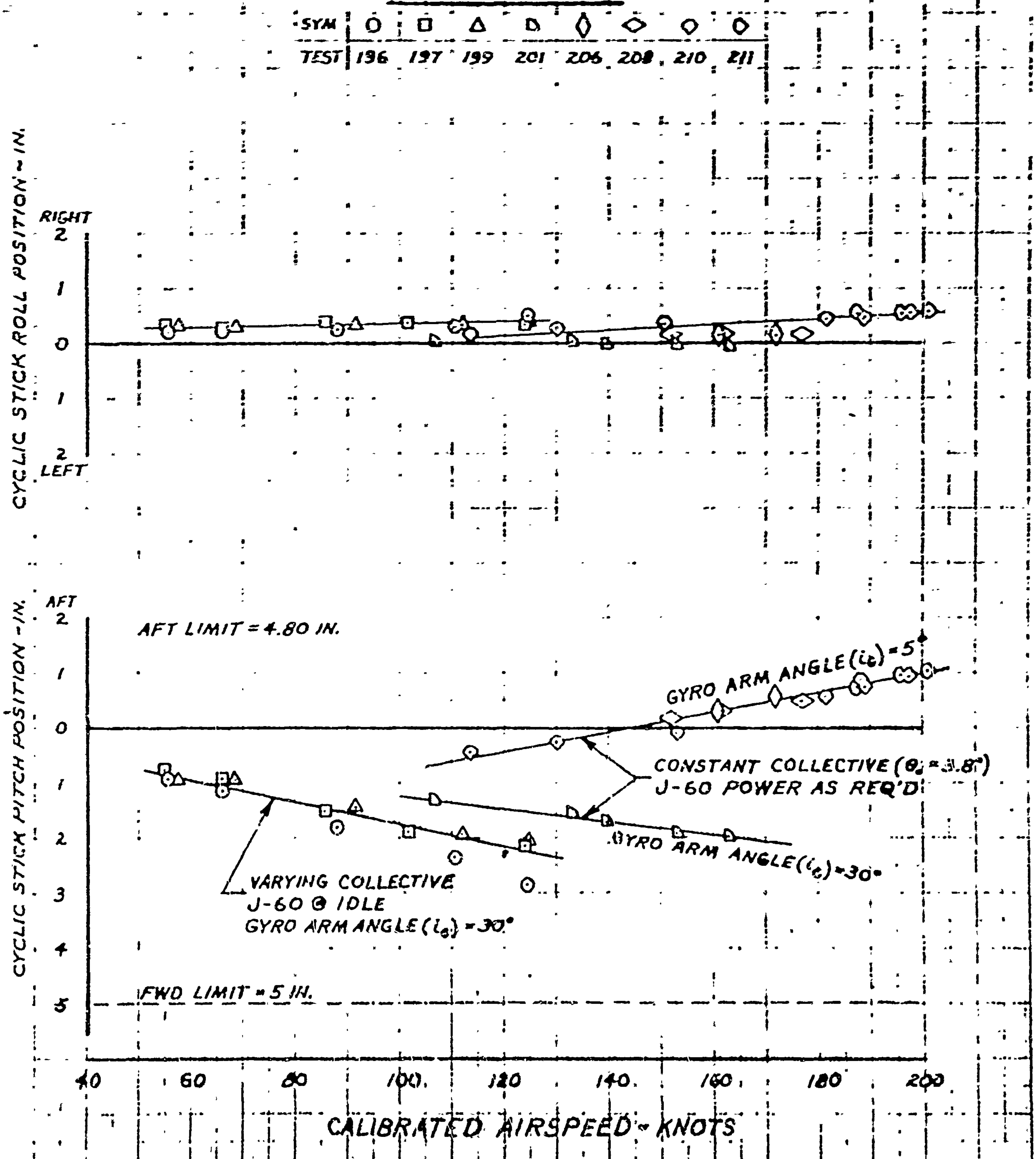

(1002 C)

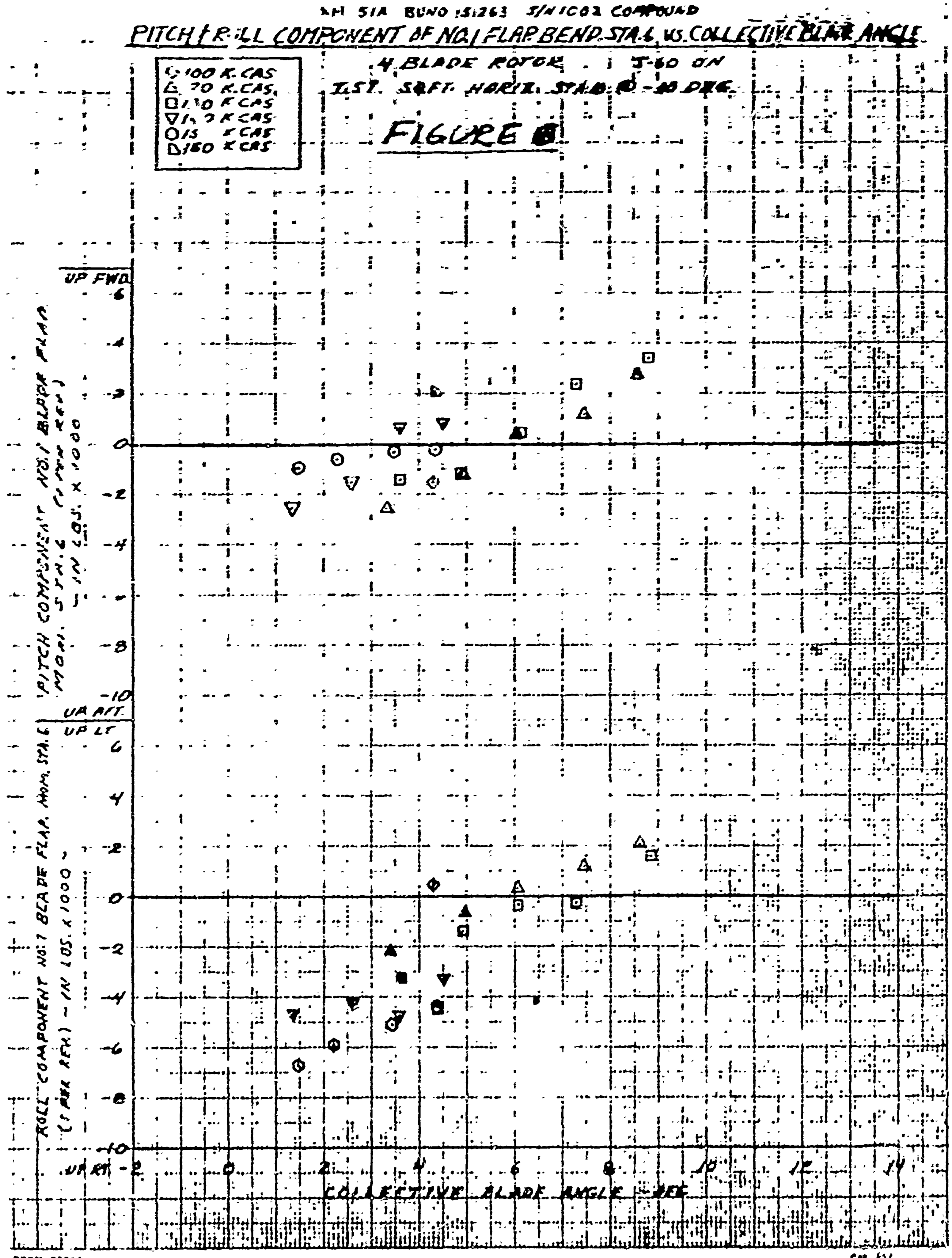
AH 51A BUNO 151263 S/N 1002 COMPOUND
PITCH & ROLL COMPONENT OF NO. 1 FLAP BEND STA. 6 VS. COLLECTIVE BLADE ANGLE
4 BLADE ROTOR
J-60 ON
FIGURE
100 K. CAS
70 K. CAS
130 K CAS
150 K CAS
PITCH COMPONENT NO. 1 BLADE FLAP MOM. STA. 6 (ROTOR REF.) ~ IN LBS. X 1000
UP FWD
UP AFT
UP LT
UP RT
ROLL COMPONENT NO. 1 BLADE FLAP. MOM. STA. 6 (ROTOR REF.) ~ IN LBS. X 1000
COLLECTIVE BLADE ANGLE ~ DEG
FORM

XH-51A BUNO 151263 S/N 1008 COMPOUND

ROLL & PITCH COMPONENT VS. COLLECTIVE BLADE ANGLE

4 BLADE ROTOR

24.2 SQ. FT. HORIZ. STAB. @ 0.0 DEG.

I-62 ON

FIGURE 7

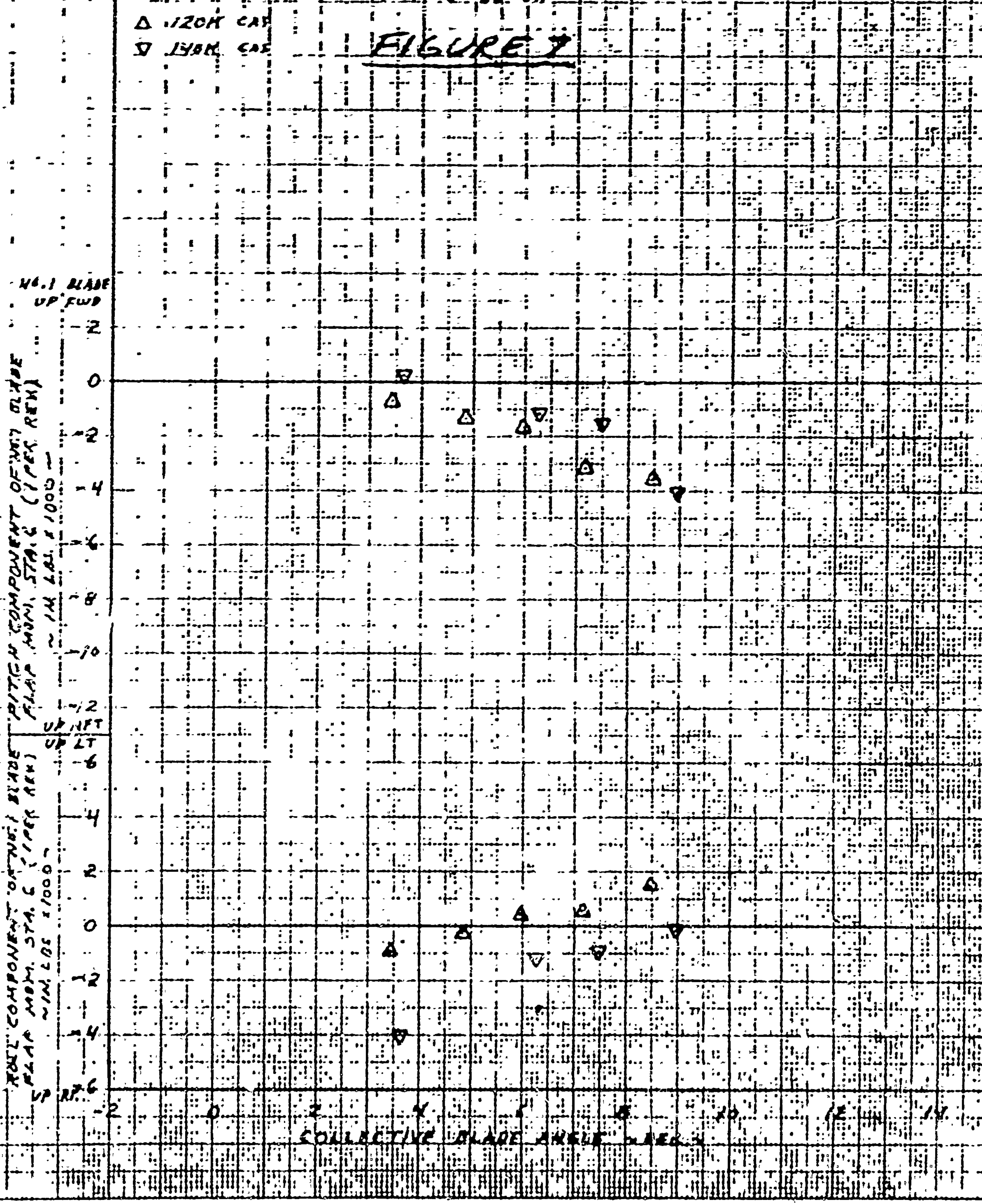

LOCKHEED HELICOPTER
MODEL XH-51A
SHIP - BUNO 151263

TAIL ROTOR PEDAL POSITION IN LEVEL FLIGHT COMPOUND HELICOPTER

FIGURE 8

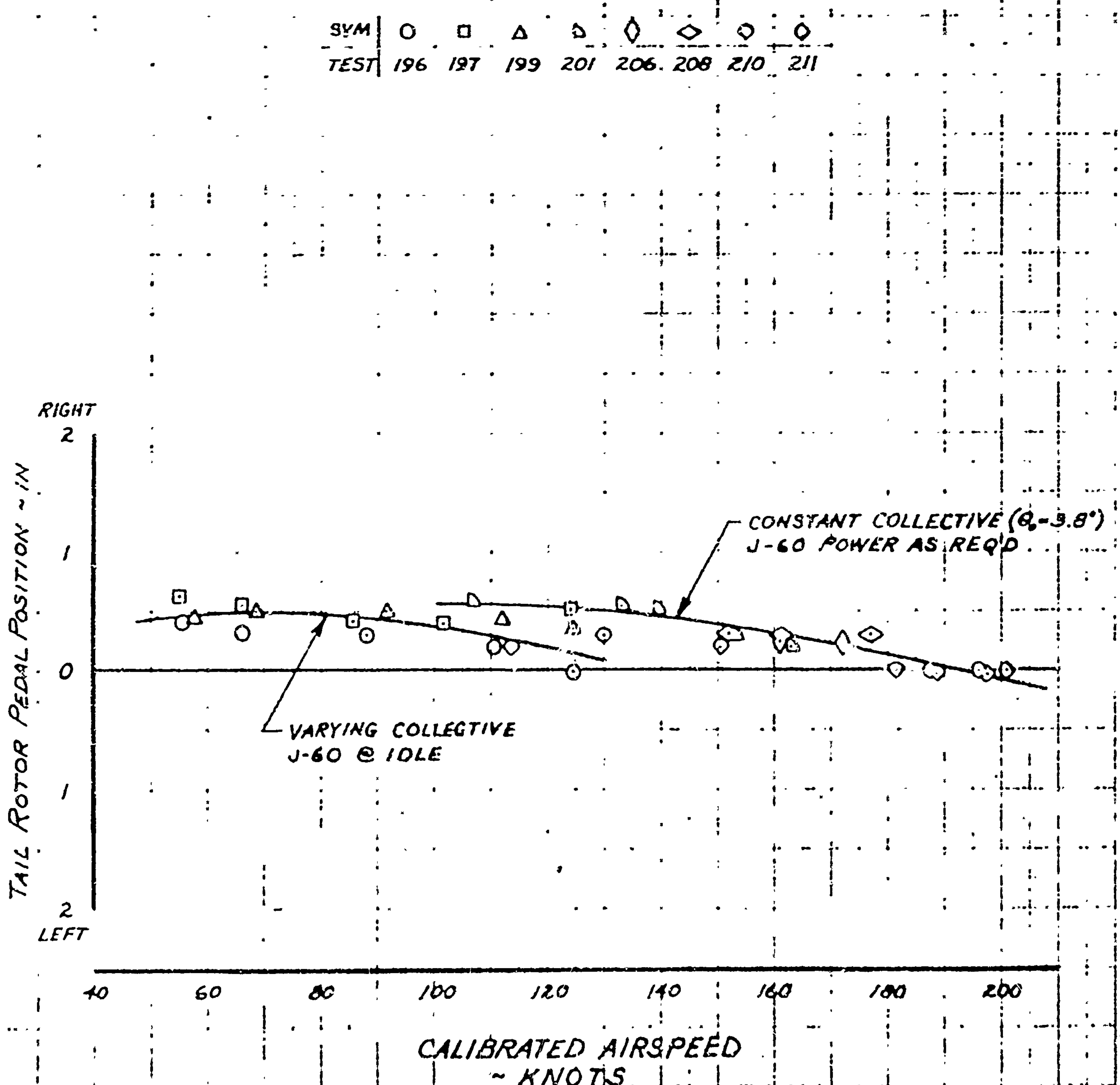

LOCKHEED HELICOPTER

MODEL XH-51A

MANEUVERING STABILITY-COMPOUND HELICOPTER

J-60 ENGINE OPERATING

SHIP: BUNO 151263

FIGURE 9

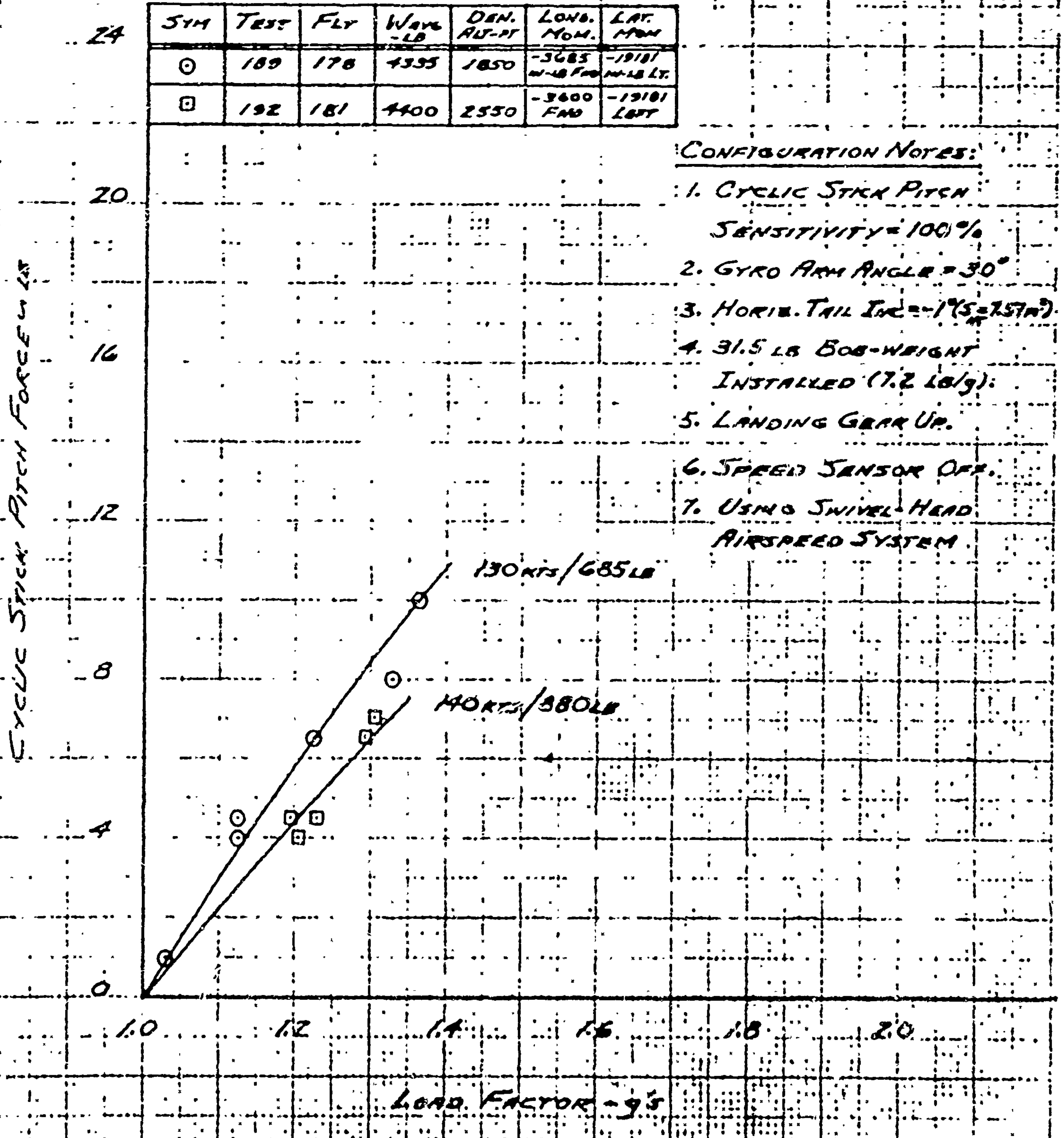

SYM	TEST	FLT	WAVG -LB	DEN. ALT-FT	LONG. MOM.	LAT. MOM.
⊙	189	178	4335	1850	-3685 IN-LB FWD	-19181 IN-LB LT.
⊡	192	181	4400	2550	-3600 FWD	-19181 LEFT

(θ_s = -3.8°)

(100% C)

FORM 8278

(100% C)

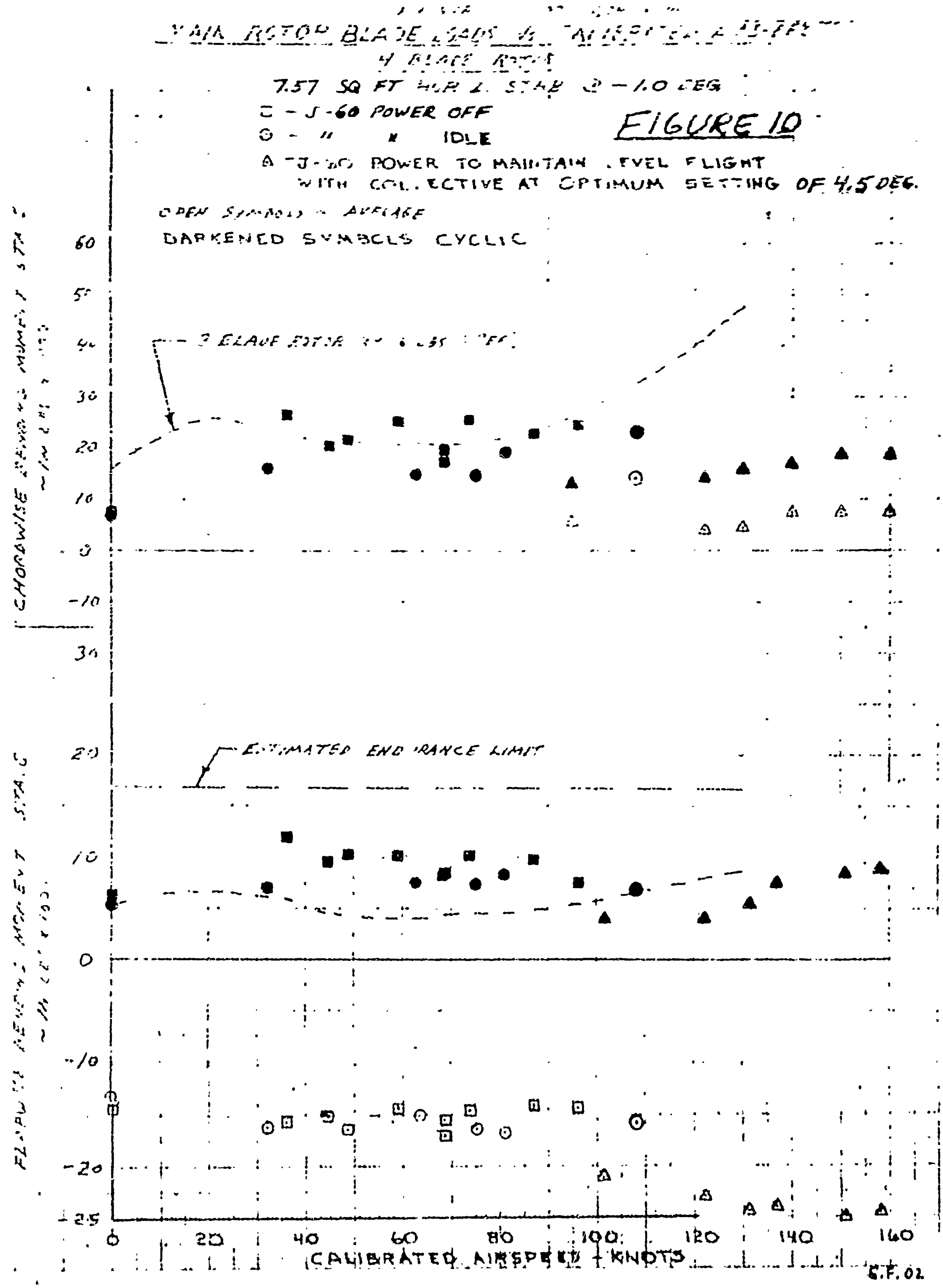

FIGURE 10

E.F. 02

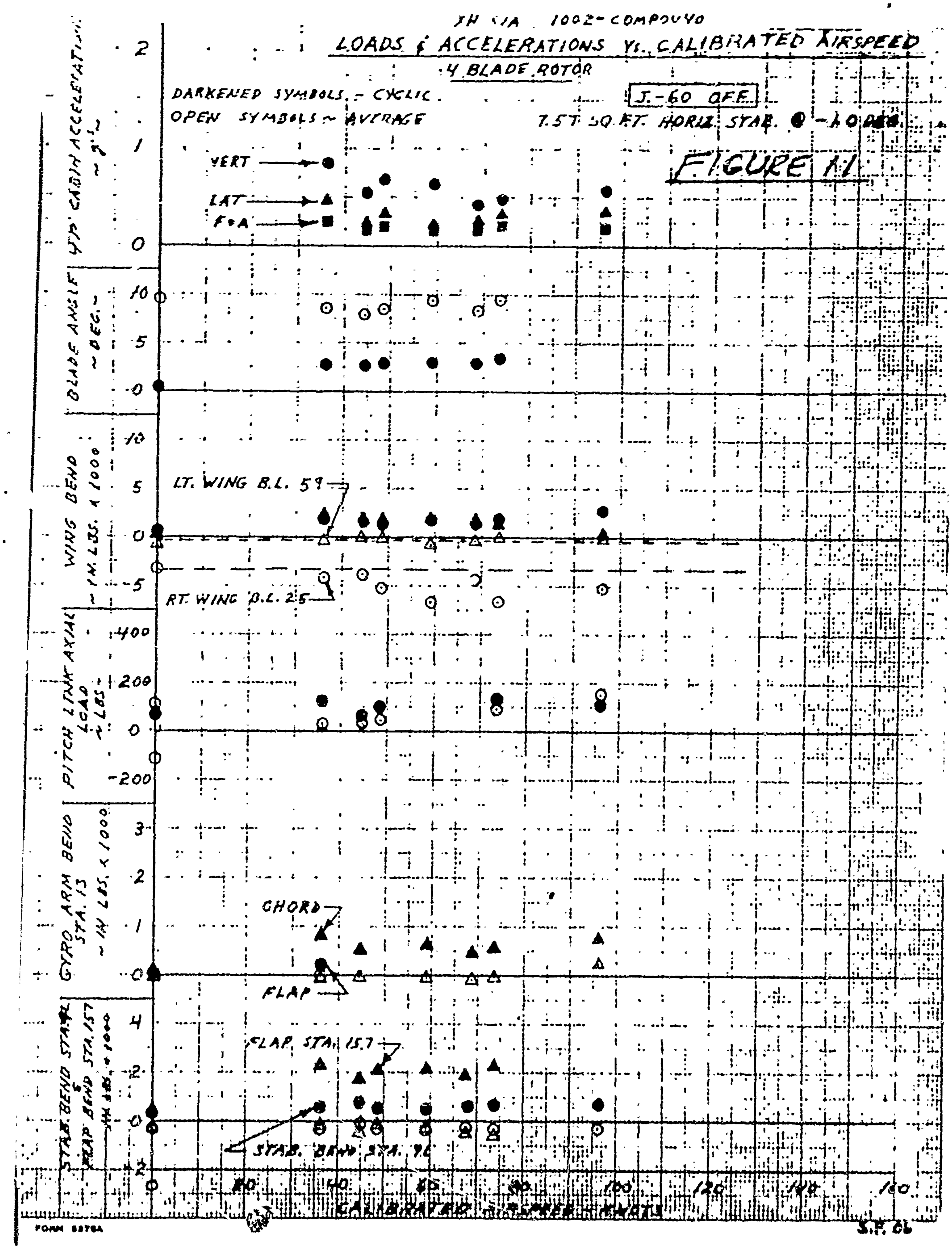
XH 51A 1002-COMPOUND
LOADS & ACCELERATIONS VS. CALIBRATED AIRSPEED
4 BLADE ROTOR
DARKENED SYMBOLS - CYCLIC.
OPEN SYMBOLS ~ AVERAGE
J-60 OFF
7.5 SQ. FT. HORIZ. STAB. @ -10 DEG
FIGURE 11
VERT
LAT
F+A
4/P CABIN ACCELERATION ~ g's
BLADE ANGLE ~ DEG.
WING BEND ~ IN. LBS. x 1000
LT. WING B.L. 59
RT. WING B.L. 25
PITCH LINK AXIAL LOAD ~ LBS.
GYRO ARM BEND STA. 13 ~ IN. LBS. x 1000
CHORD
FLAP
STAB. BEND STA. 76 & FLAP BEND STA. 157 ~ IN. LBS. x 1000
FLAP. STA. 157
STAB. BEND STA. 76
CALIBRATED AIRSPEED ~ KNOTS
20 40 60 80 100 120 140 160
S.P. 66
FORM 8878A

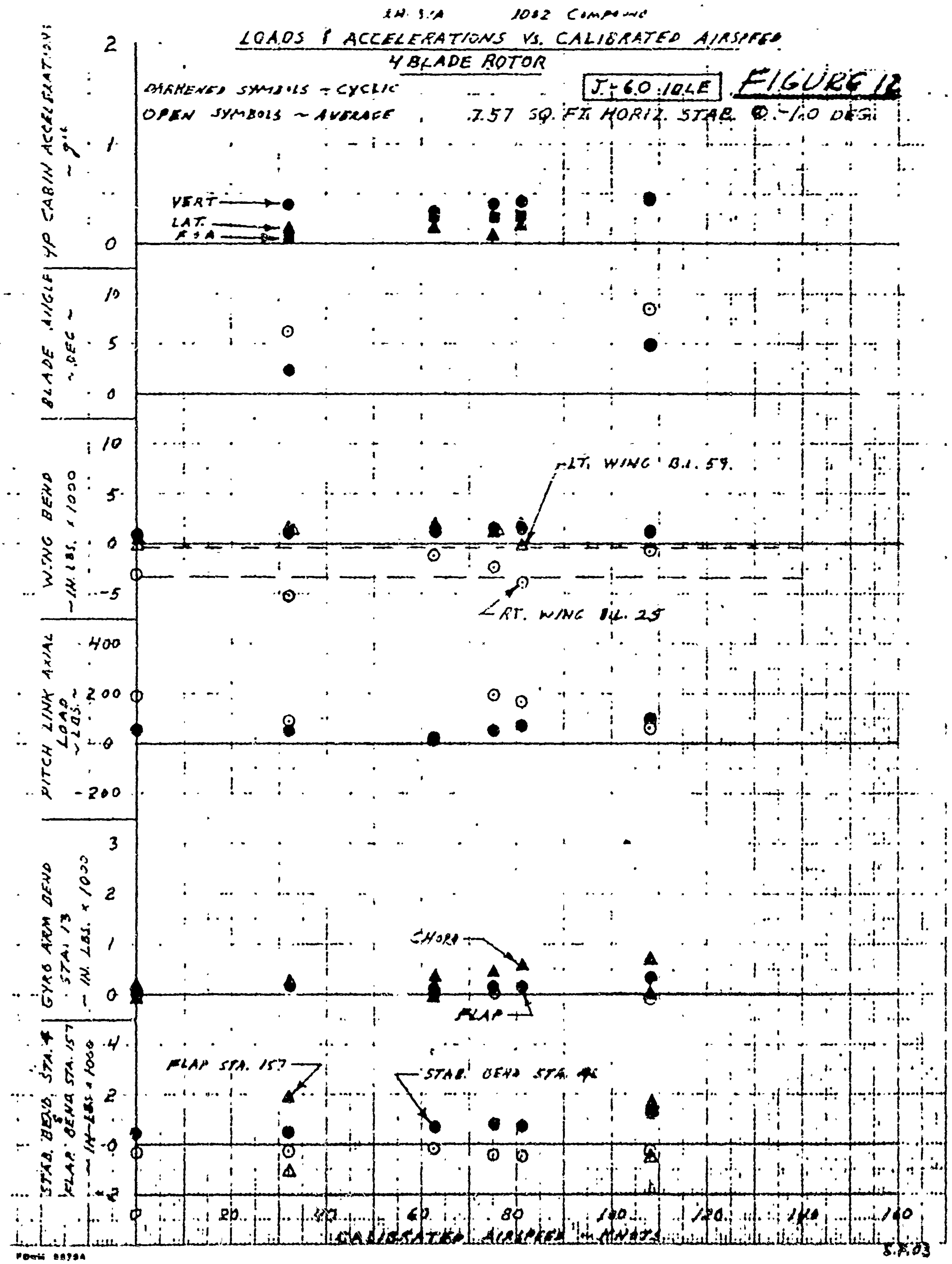
LOADS & ACCELERATIONS VS. CALIBRATED AIRSPEED
4 BLADE ROTOR
J-60 IDLE
FIGURE 12
DARKENED SYMBOLS ~ CYCLIC
OPEN SYMBOLS ~ AVERAGE
7.57 SQ. FT. HORIZ. STAB.
YP CABIN ACCELERATIONS ~ g's
VERT
LAT.
F & A
BLADE ANGLE ~ DEG ~
WING BEND ~ IN. LBS. x 1000
LT. WING B.L. 59.
RT. WING B.L. 25
PITCH LINK AXIAL LOAD ~ LBS. ~
GYRO ARM BEND STA. 13 ~ IN. LBS. x 1000
CHORD
FLAP
STAB. BEND. STA. 4 & FLAP. BEND STA. 157 ~ IN-LBS x 1000
FLAP STA. 157
STAB. BEND STA. 4
CALIBRATED AIRSPEED ~ KNOTS
0
20
40
60
80
100
120
140
160
FORM 8879A

MPOUND

MAIN ROTOR BLADE LOADS vs. COLLECTIVE

4 BLADE ROTOR

J-60 ON

HORIZ. STAB.

@ -1.0 DEG.

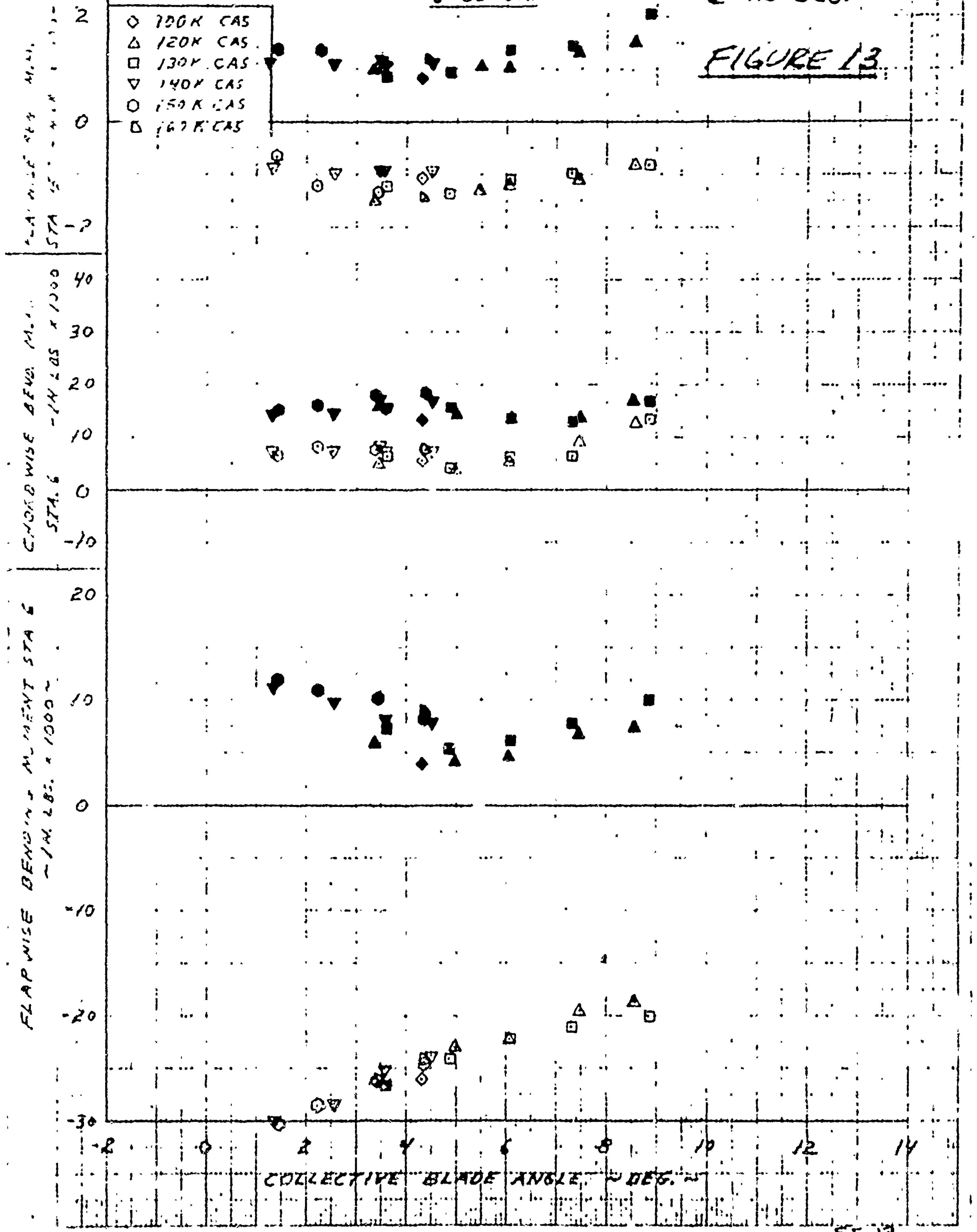

FIGURE 13

SF 13

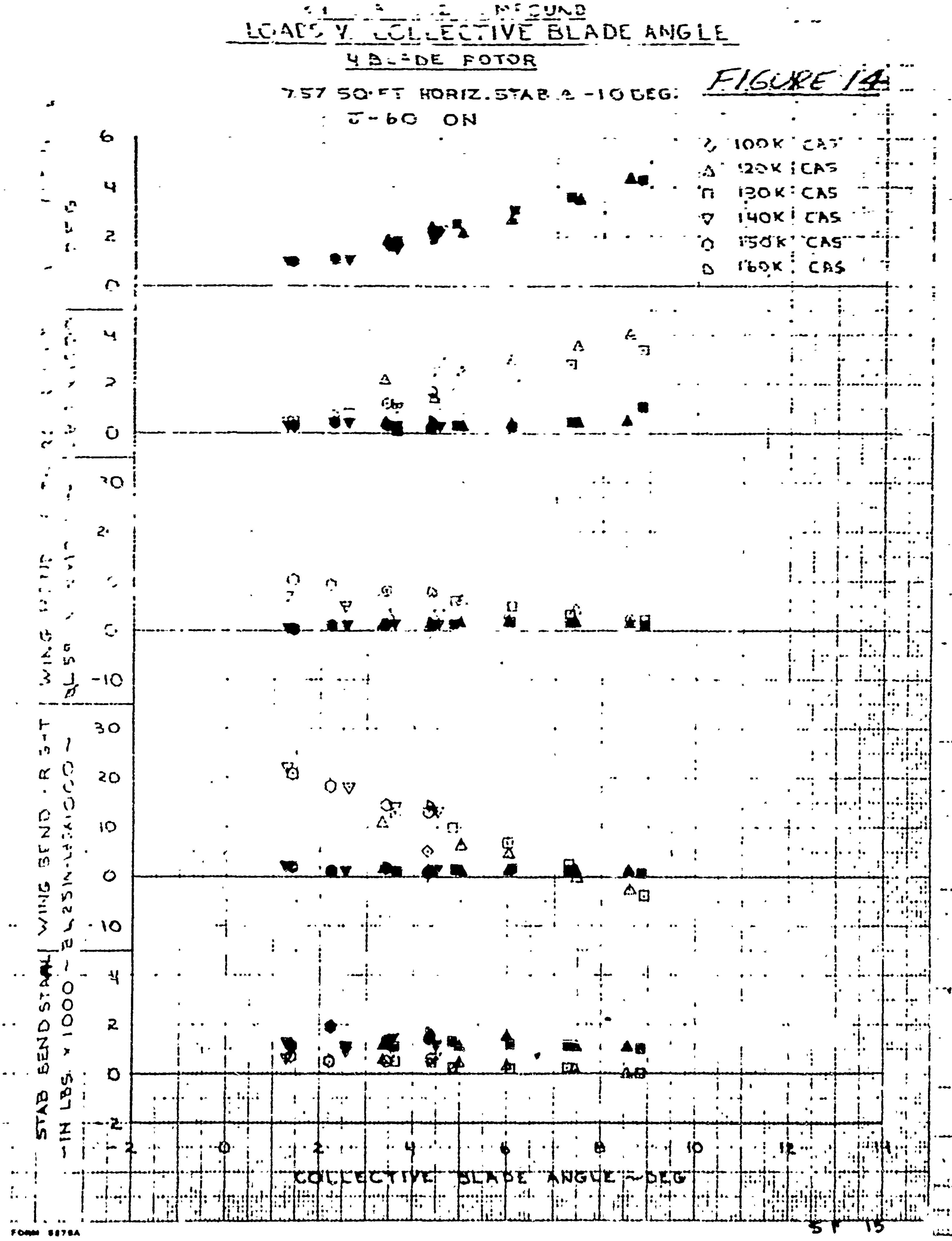
LOADS V. COLLECTIVE BLADE ANGLE
4 BLADE ROTOR
7.57 SQ FT HORIZ. STAB. @ -10 DEG.
J-60 ON
FIGURE 14
100K CAS
120K CAS
130K CAS
140K CAS
150K CAS
160K CAS
STAB BEND STA
WING BEND
COLLECTIVE BLADE ANGLE ~ DEG

XH-51A OC2 COMPOUND

LOAD VS COLLECTIVE BLADE ANGLE

4 BLADE ROTOR

FIGURE 15

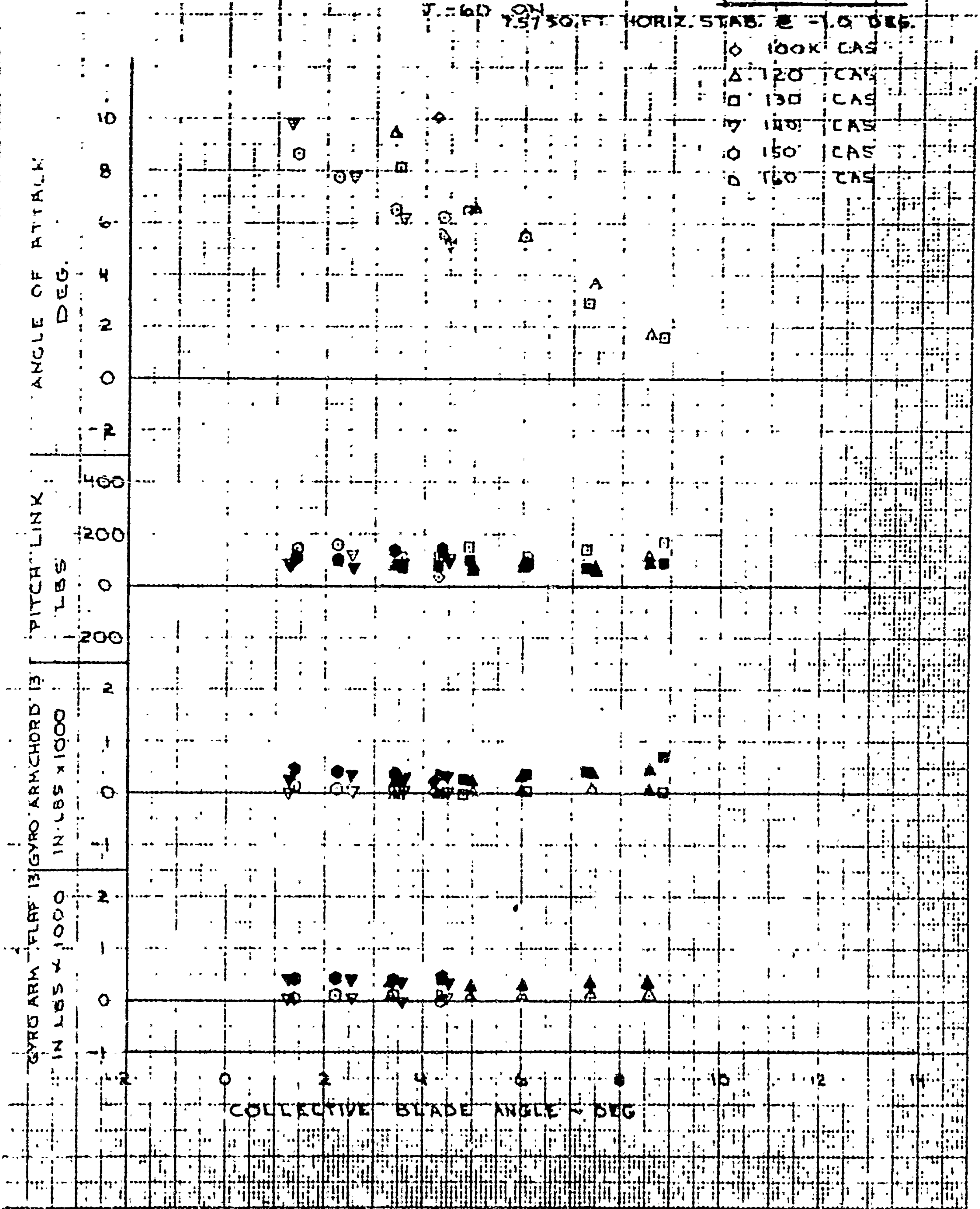

FORM 3878A

57 16

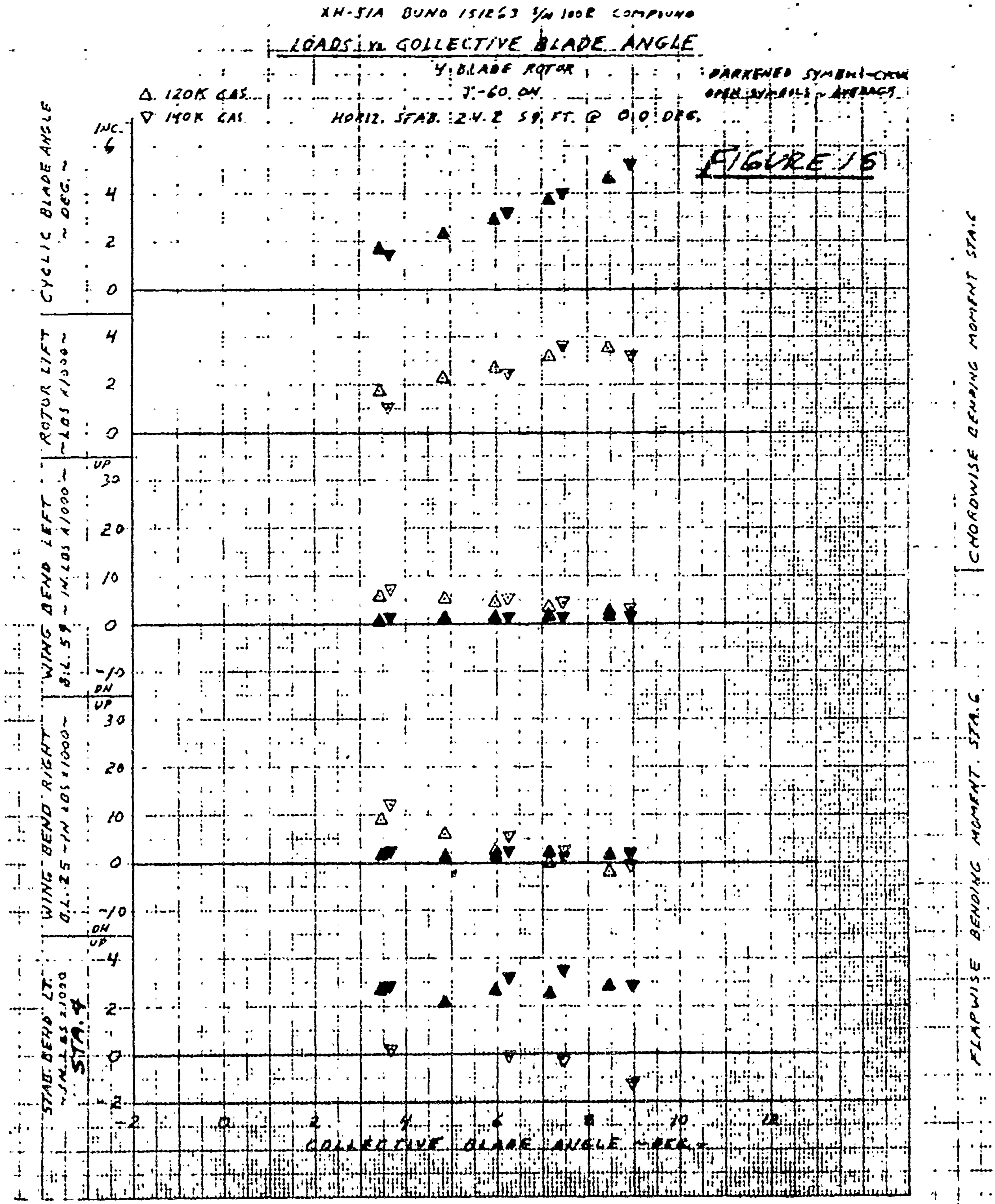
XH-51A BUNO 151263 S/N 1002 COMPOUND
LOADS vs COLLECTIVE BLADE ANGLE
4 BLADE ROTOR
J-60 ON
HORIZ. STAB. 24.2 SQ. FT. @ 0.0 DEG.
Δ 120K CAS
∇ 140K CAS
DARKENED SYMBOL - CYCLIC
OPEN SYMBOLS - AVERAGE
FIGURE 16
CYCLIC BLADE ANGLE ~ DEG. ~
ROTOR LIFT ~LBS X1000~
WING BEND LEFT B.L. 59 ~ IN.LBS X1000~
WING BEND RIGHT B.L. 25 ~ IN LBS X1000~
STAB. BEND LT. ~ IN. LBS X1000
STA. 4
CHORDWISE BENDING MOMENT STA.6
FLAPWISE BENDING MOMENT STA.6
COLLECTIVE BLADE ANGLE ~ DEG.

FORM 8878A

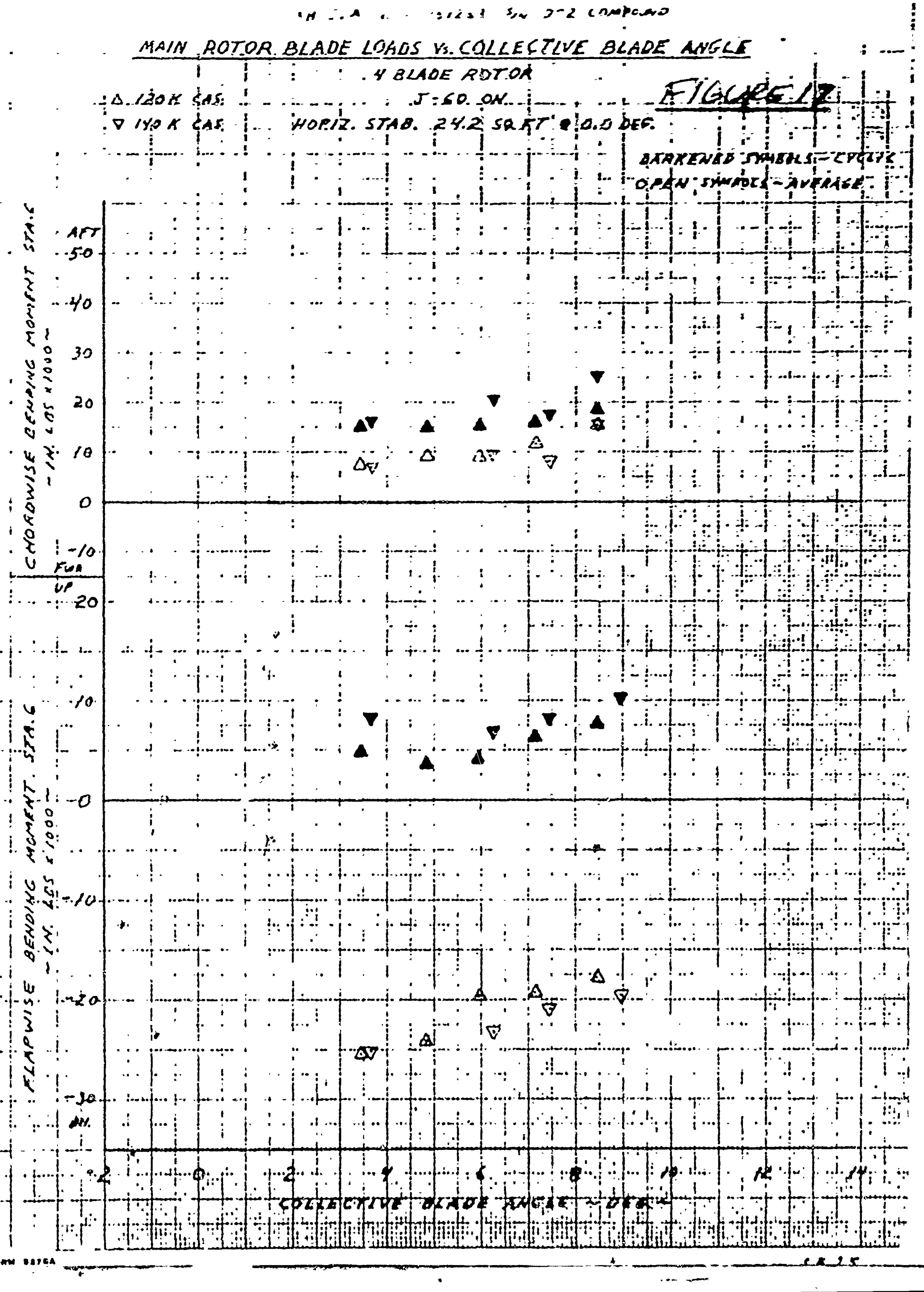

MAIN ROTOR BLADE LOADS Vs. COLLECTIVE BLADE ANGLE
4 BLADE ROTOR
J-60 ON
HORIZ. STAB. 24.2 SQ.FT @ 0.0 DEG.
FIGURE 12
△ 120 K CAS
▽ 140 K CAS
DARKENED SYMBOLS – CYCLIC
OPEN SYMBOLS – AVERAGE
CHORDWISE BENDING MOMENT STA.6 ~IN. LBS x1000~
AFT
FWD
UP
DN.
FLAPWISE BENDING MOMENT STA.6 ~IN. LBS x1000~
COLLECTIVE BLADE ANGLE ~ DEG

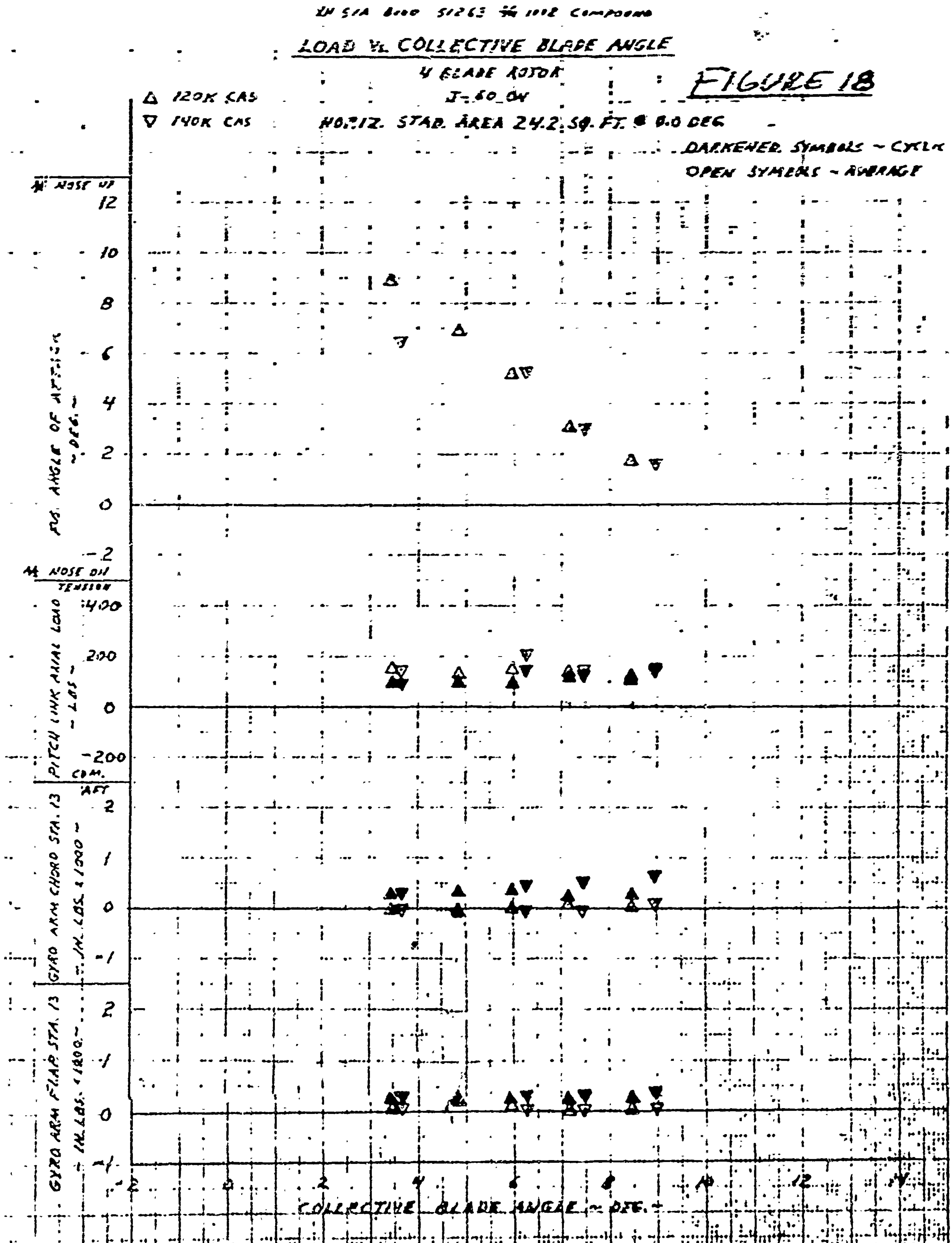

LOAD Vs. COLLECTIVE BLADE ANGLE
4 BLADE ROTOR
FIGURE 18
Δ 120K CAS
∇ 140K CAS
HORIZ. STAB. AREA 24.2 SQ. FT. @ 0.0 DEG
DARKENED SYMBOLS ~ CYCLIC
OPEN SYMBOLS ~ AVERAGE
NOSE UP
NOSE DN
TENSION
COM.
AFT
PITCH LINK AXIAL LOAD ~ LBS ~
GYRO ARM CHORD STA. 13
GYRO ARM FLAP STA. 13
COLLECTIVE BLADE ANGLE ~ DEG.

FORM 88794

XH 51A - 1003 COMPOUND

MAIN ROTOR BLADE LOADS VS. CALIBRATED AIRSPEED

4 BLADE ROTOR

J-60 GN.

FIGURE 19

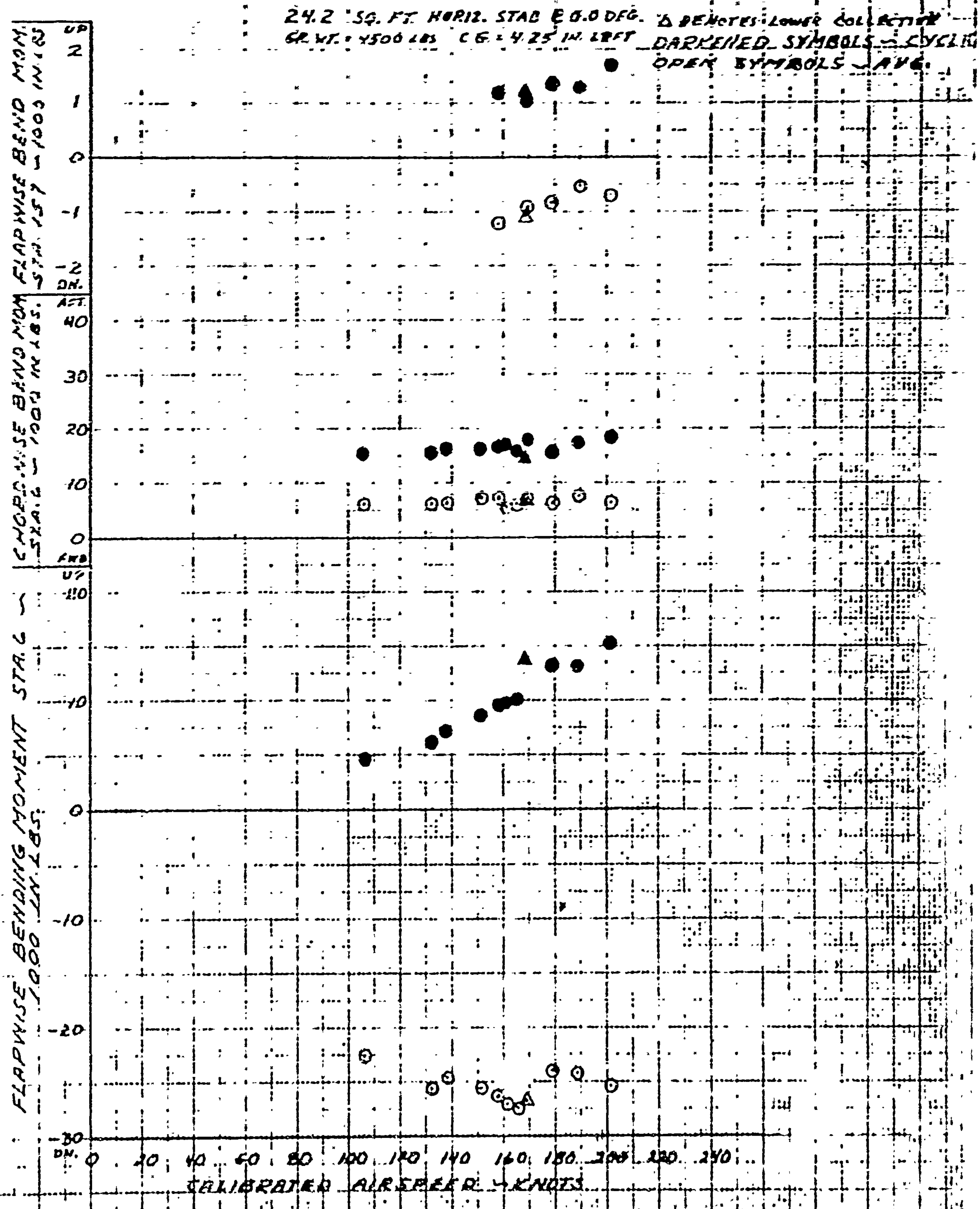

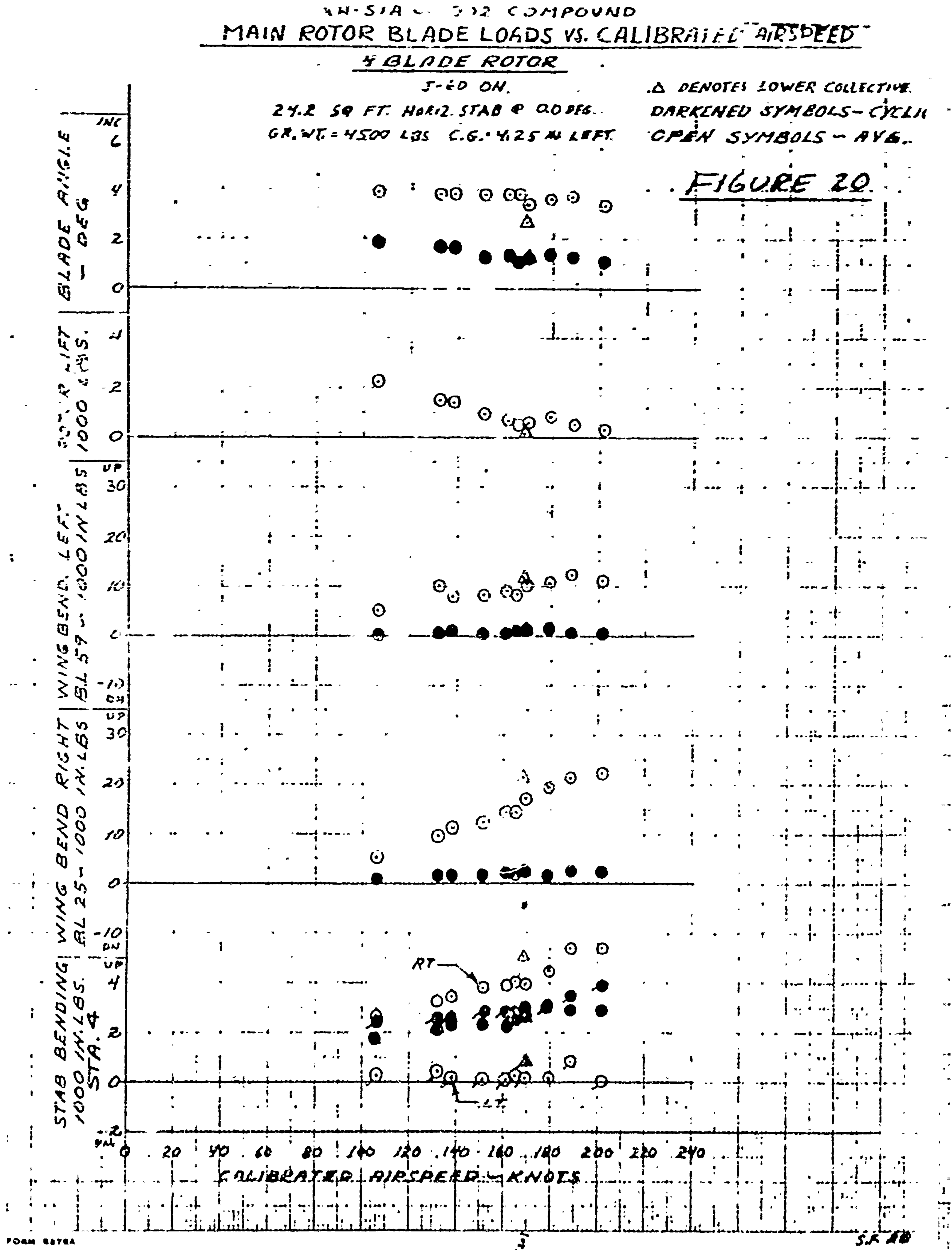
XH-51A ... 332 COMPOUND
MAIN ROTOR BLADE LOADS VS. CALIBRATED AIRSPEED
4 BLADE ROTOR
J-60 ON.
24.2 SQ FT. HORIZ. STAB @ 0.0 DEG.
GR. WT. = 4500 LBS C.G. 4.25 IN LEFT
Δ DENOTES LOWER COLLECTIVE
DARKENED SYMBOLS - CYCLIC
OPEN SYMBOLS - AVG.
FIGURE 20
BLADE ANGLE - DEG
WING BEND. LEFT BL 59 - 1000 IN.LBS
WING BEND RIGHT BL 25 - 1000 IN.LBS
STAB BENDING 1000 IN.LBS. STA. 4
RT
LT
CALIBRATED AIRSPEED - KNOTS
0 20 40 60 80 100 120 140 160 180 200 220 240
FORM 5578A
S.K.

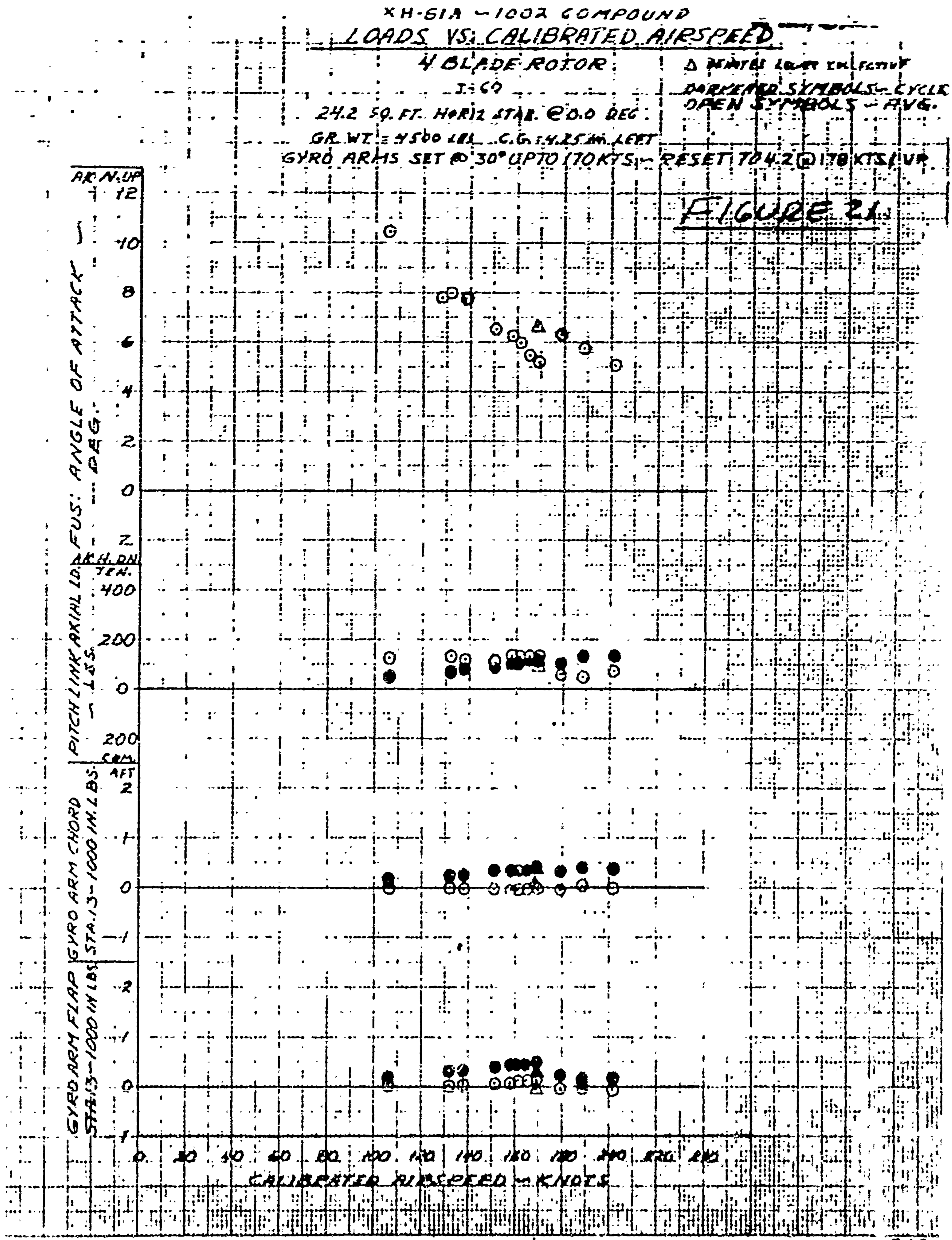
XH-51A - 1002 COMPOUND
LOADS VS. CALIBRATED AIRSPEED
4 BLADE ROTOR
24.2 SQ. FT. HORIZ STAB. @ 0.0 DEG
GR. WT. = 4500 LBS. C.G. = 4.25 in. LEFT
GYRO ARMS SET @ 30° UP TO 170 KTS - RESET TO 4.2 @ 178 KTS & UP
DARKENED SYMBOLS - CYCLIC
OPEN SYMBOLS - AVG.
FIGURE 21
FUS. ANGLE OF ATTACK - DEG.
AR. N. UP
AR. N. DN
PITCH LINK AXIAL LD. - LBS.
TEN.
COM.
GYRO ARM CHORD STA. 13 - 1000 IN. LBS.
AFT
GYRO ARM FLAP STA. 13 - 1000 IN. LBS.
CALIBRATED AIRSPEED ~ KNOTS

SH-51A B.N. [illegible] 263 S/N 1002 COMPOUND

TAIL ROTOR FLAP BEND STA 19.5 vs CALIBRATED AIRSPEED

4 BLADE ROTOR

J-60.04

FIGURE 22

HORIZ. STAB. AREA 24.2 SQ. FT. @ 0.0 DEG.

GR. WT = 4500 LBS C.G. 4.25 IN. LEFT

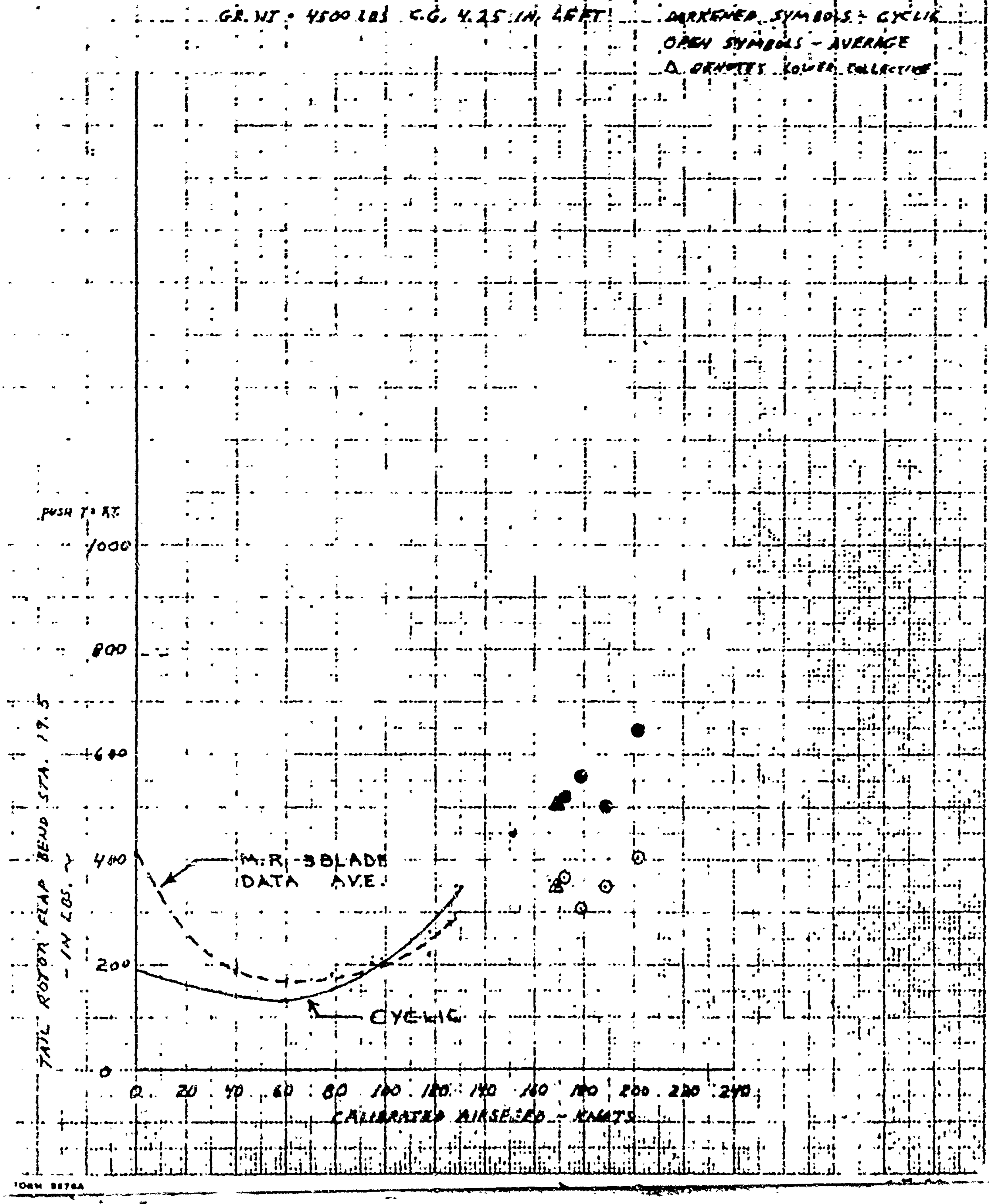

XH-51A BUNO 151263 S/N 1002 COMPOUND

ROLL & PITCH COMPONENT vs. CALIBRATED AIRSPEED

4 BLADE ROTOR.

24.2 SQ. FT. HORIZ. STAB. @ 0.0 DEG.

GR. WT. = 4540 LBS. C.G. = 4.25 IN. LEFT

Δ DENOTES LOWER COLLECTIVE

J-60 ON

FIGURE 22

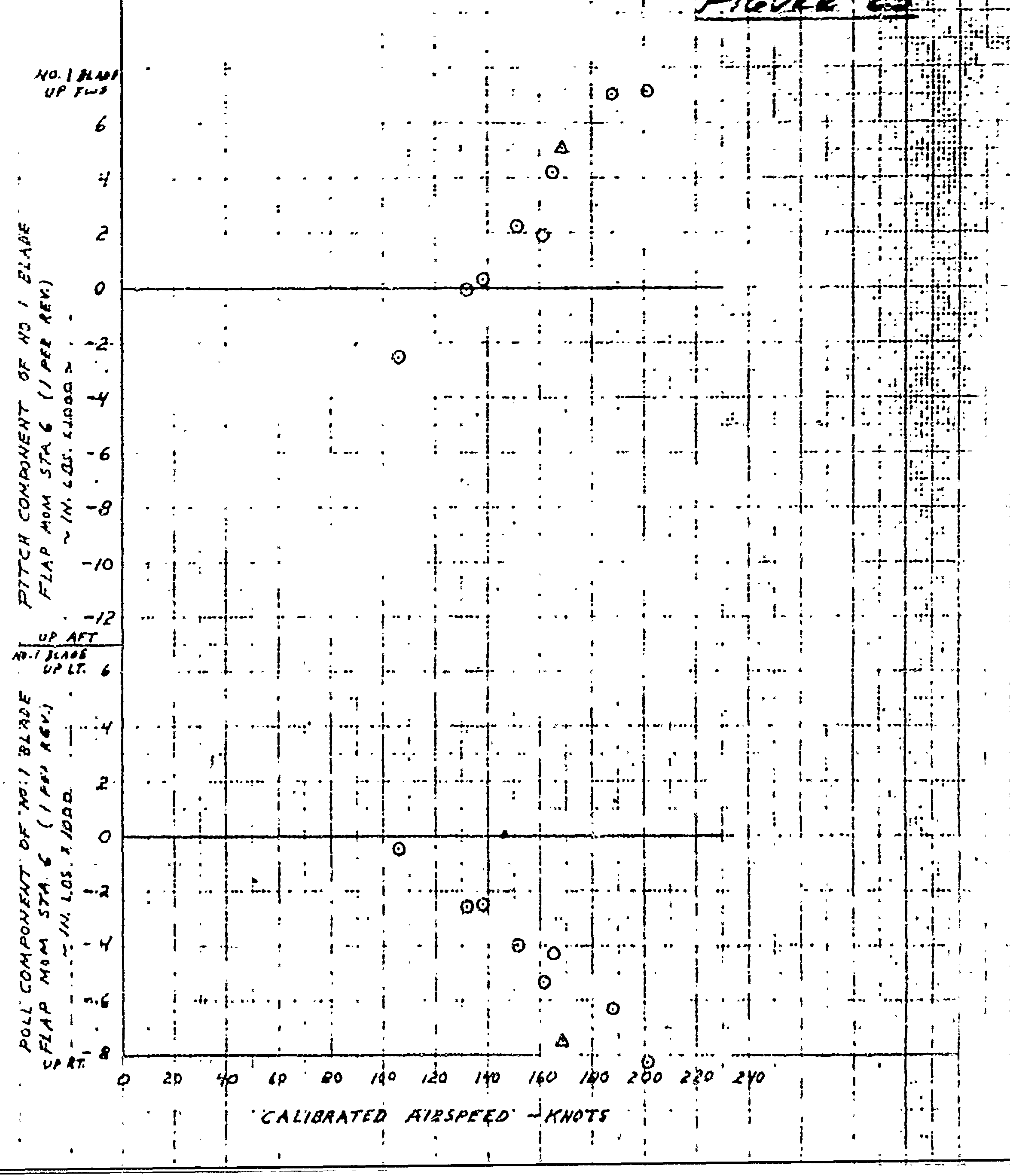

XH-51A BUNO 151263 S/N 1002 COMPOUND

V-N DIAGRAM

GROSS WT. ~ 4300 LBS. C.G. ~ 0.8 IN. FWD. ~ 4.4 IN. LT.

J-60 OFF

FIGURE 24

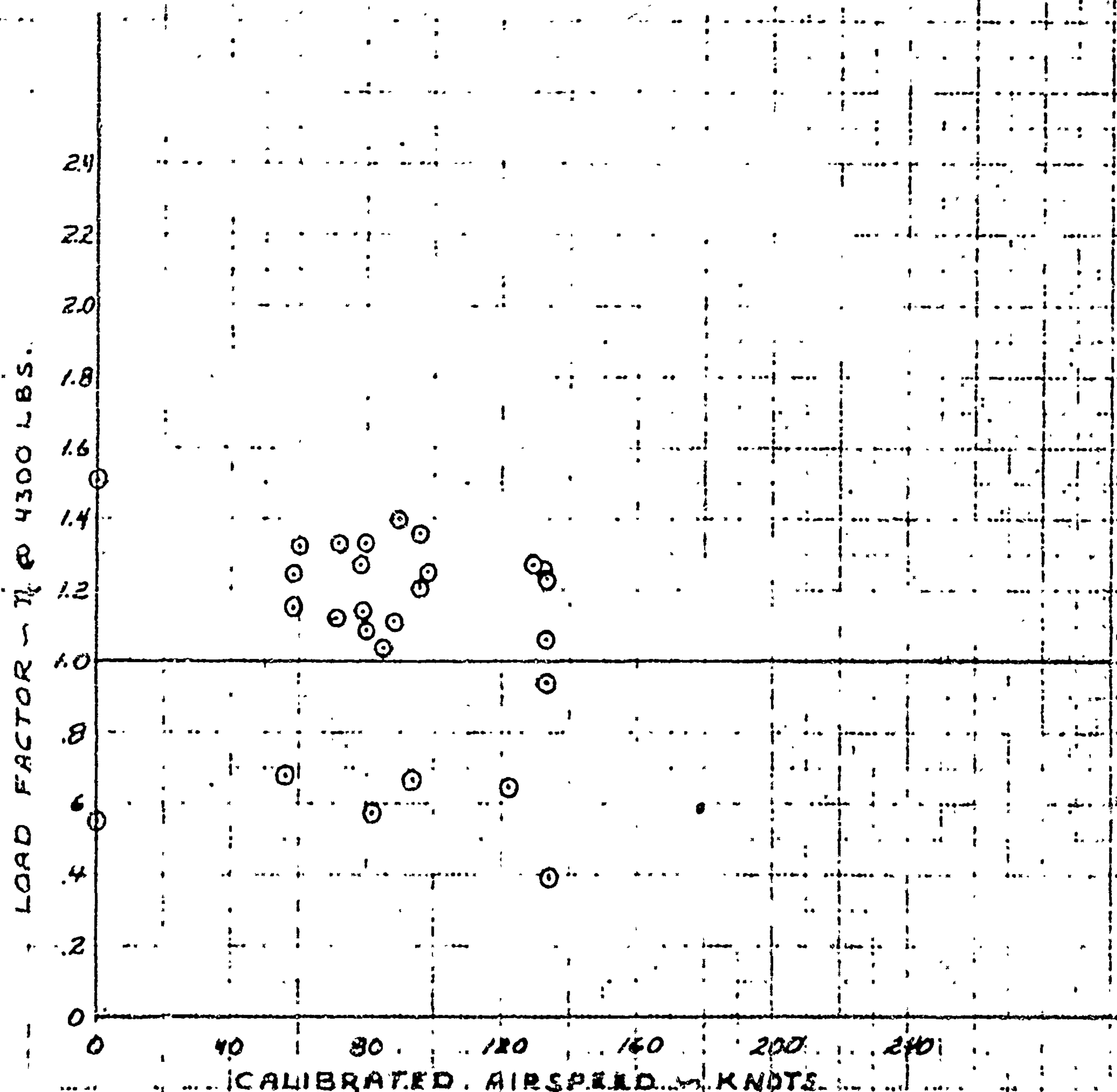

FORM 4473A

XH-51A BUNO 151263 S/N 1002 COMPOUND

V-N DIAGRAM

GROSS WEIGHT ~ 4300 LBS C.G. ~ 4.25 IN. LEFT

J-60 ON

FIGURE 25

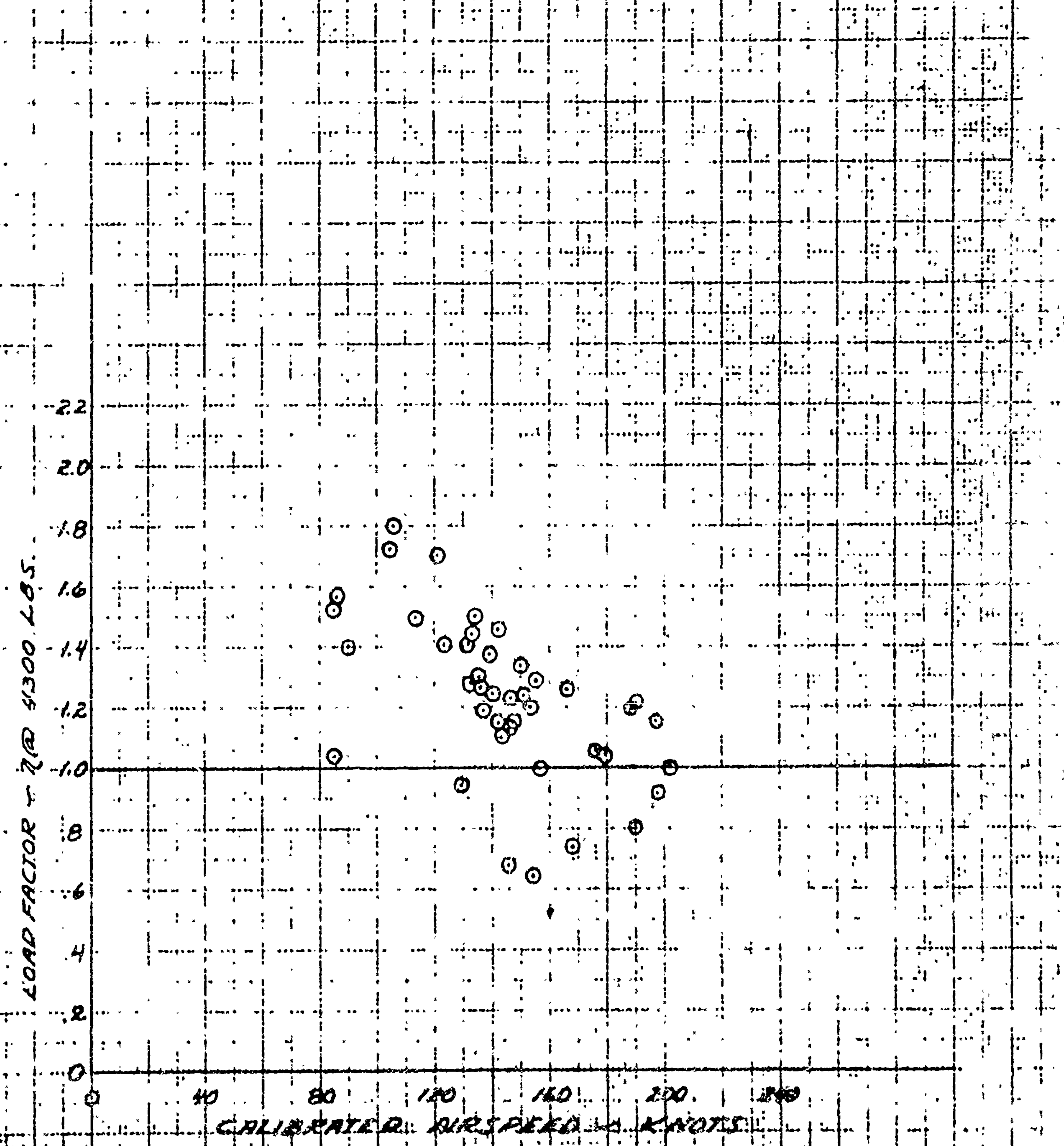

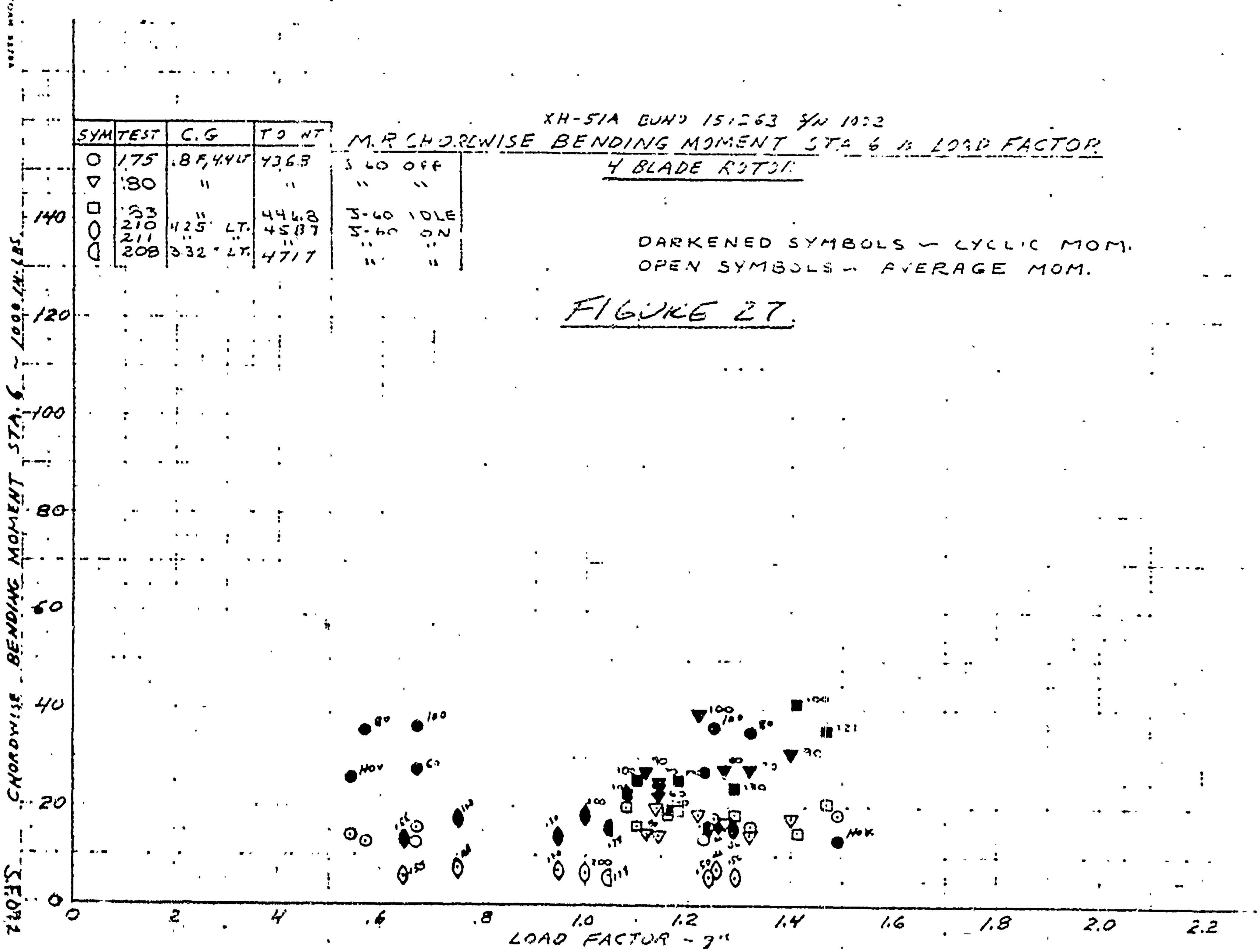
XH-51A BUNO 151263 S/N 1002
M.R. CHORDWISE BENDING MOMENT STA 6 vs LOAD FACTOR
4 BLADE ROTOR
SYM TEST C.G TO WT
○ 175 .8 F, 4.4 LT 4368 3-60 OFF
▽ 180 " " " "
□ 153 " 4468 3-60 IDLE
⬯ 210 211 4.25 LT. 4587 3-60 ON
⬯ 208 3.32 LT. 4717 " "
DARKENED SYMBOLS ~ CYCLIC MOM.
OPEN SYMBOLS ~ AVERAGE MOM.
CHORDWISE BENDING MOMENT STA. 6 ~ 1000 IN-LBS.
LOAD FACTOR ~ g's

FIGURE 27.

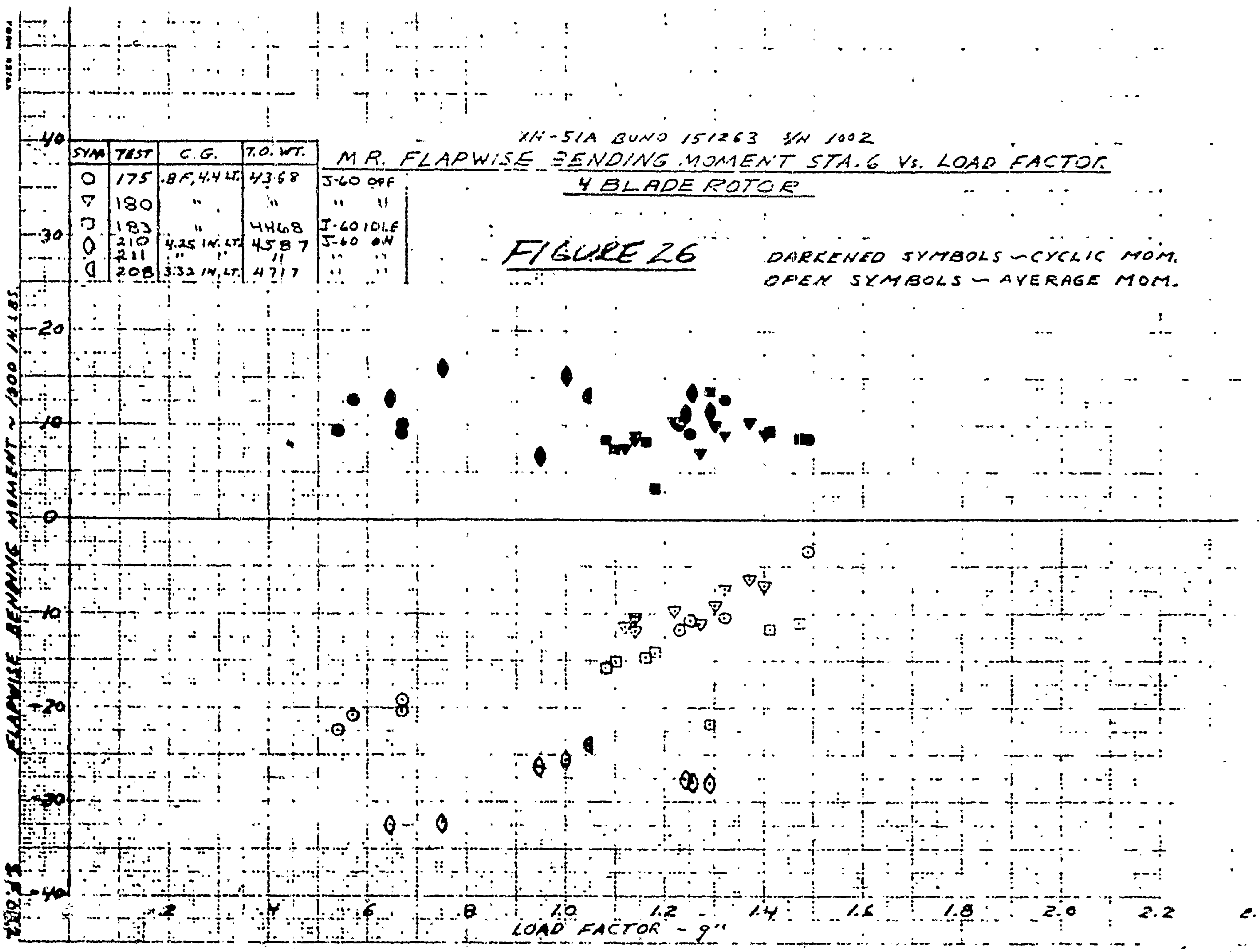
XH-51A BUNO 151263 S/N 1002
M.R. FLAPWISE BENDING MOMENT STA. 6 Vs. LOAD FACTOR
4 BLADE ROTOR
SYM TEST C.G. T.O. WT.
175 .8F, 4.4 LT. 4368 J-60 OFF
180 " " " "
183 " 4468 J-60 IDLE
210 4.25 IN. LT. 4587 J-60 ON
211 " " " " "
208 3.32 IN. LT. 4717 " "
DARKENED SYMBOLS ~ CYCLIC MOM.
OPEN SYMBOLS ~ AVERAGE MOM.
FLAPWISE BENDING MOMENT ~ 1000 IN. LBS.
40
30
20
10
0
10
20
30
40
.2
.4
.6
.8
1.0
1.2
1.4
1.6
1.8
2.0
2.2
2.4
LOAD FACTOR - g''

FIGURE 26

XH-51A BUNO 151263 S/N 1002 COMPOUND

MR FLAPWISE BENDING MOMENT STA 157 Vs LOAD FACTOR

4 BLADE ROTOR

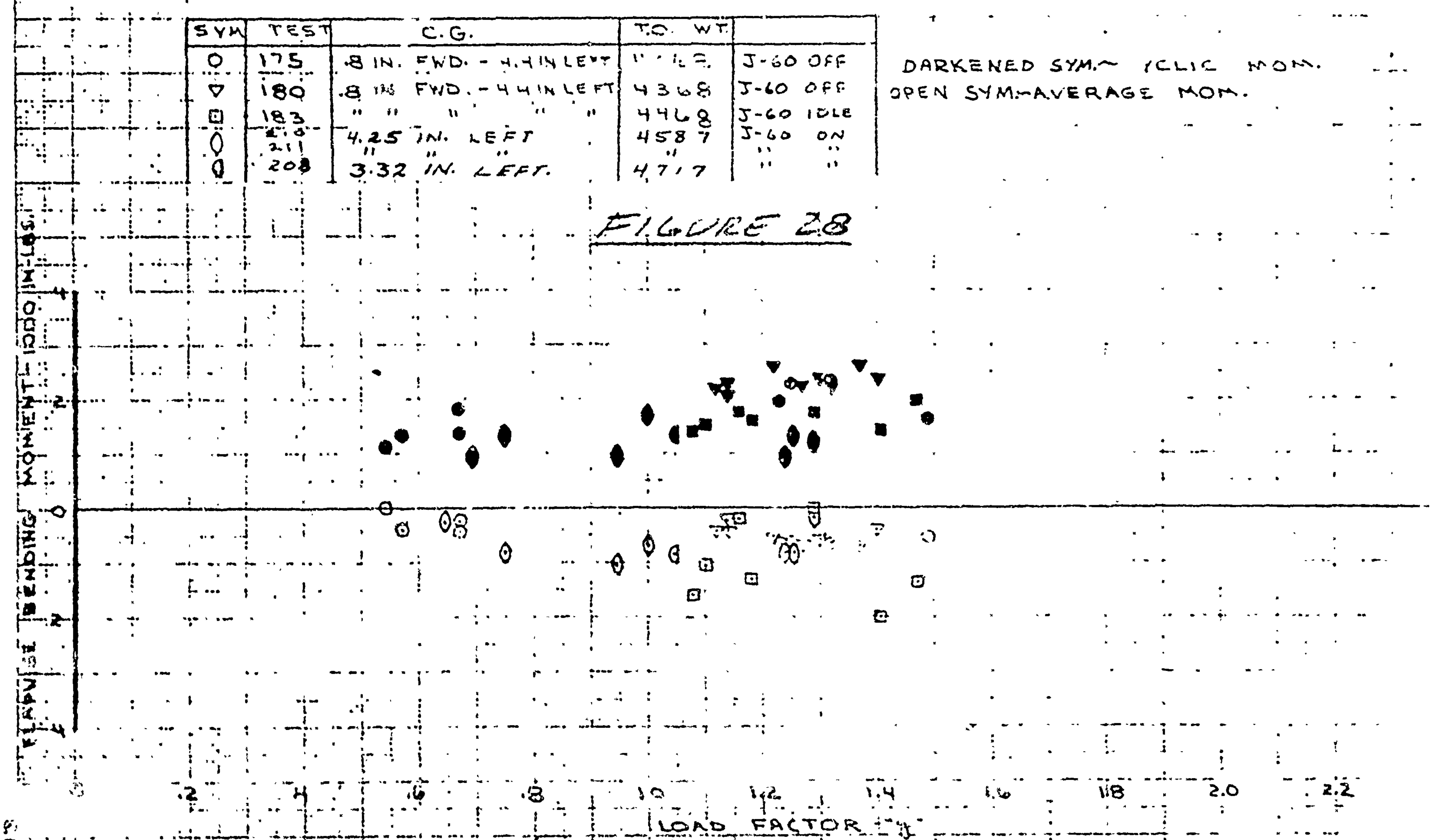

FIGURE 28

XH-51A BUNO 151263 S/N 1002 COMP.

CABIN VIBRATIONS VS. CALIBRATED AIRSPEED

4 BLADE ROTOR

FIGURE 29